

Interpreting top-quark LHC measurements in the standard-model effective field theory

J. A. Aguilar Saavedra,¹ C. Degrande,² G. Durieux,³
 F. Maltoni,⁴ E. Vryonidou,² C. Zhang⁵ (editors),
 D. Barducci,⁶ I. Brivio,⁷ V. Cirigliano,⁸ W. Dekens,^{8,9} J. de Vries,¹⁰ C. Englert,¹¹
 M. Fabbrichesi,¹² C. Grojean,^{3,13} U. Haisch,^{2,14} Y. Jiang,⁷ J. Kamenik,^{15,16}
 M. Mangano,² D. Marzocca,¹² E. Mereghetti,⁸ K. Mimasu,⁴ L. Moore,⁴ G. Perez,¹⁷
 T. Plehn,¹⁸ F. Riva,² M. Russell,¹⁸ J. Santiago,¹⁹ M. Schulze,¹³ Y. Soreq,²⁰
 A. Tonerio,²¹ M. Trott,⁷ S. Westhoff,¹⁸ C. White,²² A. Wulzer,^{2,23,24} J. Zupan.²⁵

¹ Departamento de Física Teórica y del Cosmos, U. de Granada, E-18071 Granada, Spain

² CERN, Theoretical Physics Department, Geneva 23 CH-1211, Switzerland

³ DESY, Notkestraße 85, D-22607 Hamburg, Germany

⁴ Centre for Cosmology, Particle Physics and Phenomenology (CP3), Université catholique de Louvain, B-1348 Louvain-la-Neuve, Belgium

⁵ Institute of High Energy Physics, Chinese Academy of Sciences, Beijing 100049, China

⁶ SISSA and INFN, Sezione di Trieste, via Bonomea 265, 34136 Trieste, Italy

⁷ Niels Bohr International Academy and Discovery Center, Niels Bohr Institute, University of Copenhagen, DK-2100 Copenhagen, Denmark

⁸ Theoretical Division, Los Alamos National Laboratory, Los Alamos, NM 87545, USA

⁹ New Mexico Consortium, Los Alamos Research Park, Los Alamos, NM 87544, USA

¹⁰ Nikhef, Theory Group, Science Park 105, 1098 XG, Amsterdam, The Netherlands

¹¹ SUPA, School of Physics and Astronomy, University of Glasgow, Glasgow G12 8QQ, UK

¹² INFN, Sezione di Trieste, Via Valerio 2, 34127 Trieste, Italy

¹³ Institut für Physik, Humboldt-Universität zu Berlin, D-12489 Berlin, Germany

¹⁴ Rudolf Peierls Centre for Theoretical Physics, University of Oxford, OX1 3NP Oxford, UK

¹⁵ Jožef Stefan Institute, Jamova 39, 1000 Ljubljana, Slovenia

¹⁶ Faculty of Mathematics and Physics, University of Ljubljana, Jadranska 19, 1000 Ljubljana, Slovenia

¹⁷ Department of Particle Physics and Astrophysics, Weizmann Institute of Science, Rehovot 7610001, Israel

¹⁸ Institut für Theoretische Physik, Universität Heidelberg, Germany

¹⁹ CAFPE and Departamento de Física Teórica y del Cosmos, U. de Granada, E-18071 Granada, Spain

²⁰ Center for Theoretical Physics, Massachusetts Institute of Technology, Cambridge, MA 02139, USA

²¹ UNIFAL-MG, Rodovia José Aurélio Vilela 11999, 37715-400 Poços de Caldas, MG, Brazil

²² Centre for Research in String Theory, School of Physics and Astronomy, Queen Mary University of London, 327 Mile End Road, London E1 4NS, UK

²³ Institut de Théorie des Phénomènes Physiques, EPFL, Lausanne, Switzerland

²⁴ Dipartimento di Fisica e Astronomia, Università di Padova and INFN Padova, Italy

²⁵ Department of Physics, University of Cincinnati, Cincinnati, Ohio 45221, USA

Abstract

This note proposes common standards and prescriptions for the effective-field-theory interpretation of top-quark measurements at the LHC.

Contents

1	Introduction	2
2	Guiding principles	2
3	Operator definitions	3
4	Flavour assumptions	5
5	Example of EFT analysis strategy	7
6	Summary and outlook	10
A	Indicative constraints	11
B	UFO models	20
C	Flavour-, B- and L-conserving degrees of freedom	25
D	Less restrictive flavour symmetry	28
E	FCNC degrees of freedom	29

1 Introduction

Summarising efforts undertaken under the auspices of the LHC TOP Working Group, this theory note aims at establishing basic common standards for the interpretation of top-quark measurements at the LHC in the standard-model effective field theory (SMEFT).

Guiding principles are first stated ([Section 2](#)). In a nutshell, we rely on the Warsaw basis of gauge-invariant dimension-six operators, focus on the ones which give rise to top-quark interactions ([Section 3](#)) and limit ourselves to the tree level. Three different assumptions about beyond-the-standard-model (BSM) flavour structures are considered to prioritize studies among the otherwise overwhelming number of four-fermion operators ([Section 4](#)). Top-quark flavour-changing neutral currents (FCNCs) are examined separately ([Appendix E](#)). For convenience, degrees of freedom are defined from combinations of Warsaw-basis operator coefficients ([Appendices C and D](#)). They are aligned with the directions of the effective-field-theory (EFT) parameter space which appear in given processes, in interferences with standard-model (SM) amplitudes, and in top-quark interactions with some of the gauge boson mass eigenstates. Naming and normalization conventions are fixed. Indicative constraints on these degrees of freedom are compiled in [Appendix A](#). Model implementations are provided for tree-level Monte Carlo simulation ([Appendix B](#)). Finally, a simple example of analysis strategy is outlined to illustrate how the challenges of a global EFT treatment could be addressed and to identify the experimental outputs that would be useful in this case ([Section 5](#)). It rests on the common knowledge established over the years through many EFT studies in the top-quark, Higgs, electroweak or flavour sectors. The literature quoted in this note is by no means comprehensive or even representative of the fields of top-quark physics and EFTs.

2 Guiding principles

1. The so-called Warsaw basis of dimension-six operators [[1](#)] is adopted. See also Ref. [[2, 3](#)] for early discussions of top-quark related operators.
2. Our discussion exclusively concerns processes involving at least a top quark. Only operators involving such a particle are considered. Other operators affecting the considered

processes are assumed to be well constrained by measurements in processes that do not involve top quarks. This assumption may not always be justified and explicit checks should be performed. It was for instance shown that jet production sufficiently tightly constrain modifications to the triple gluon vertex [4].

3. Three different assumptions about BSM flavour structures are considered —mostly based on symmetries— to effectively reduce the overwhelming number of four-quark operators [5]. A baseline scenario is defined. Less and more restrictive assumptions are also considered. Top-quark FCNC operators are treated separately.

Minimal flavour violation in the quark sector is used in the baseline scenario, under the assumption of a unit Cabibbo-Kobayashi-Maskawa (CKM) matrix and finite Yukawa couplings only for the top and bottom quarks, i.e. we impose a $U(2)_q \times U(2)_u \times U(2)_d$ flavour symmetry among the first two generations. In the lepton sector, flavour diagonality, i.e. $[U(1)_{l+e}]^3$, is chosen as baseline.

4. For convenience, we identify the linear combinations of Warsaw-basis operators that appear in interferences with SM amplitudes and in interactions with physical fields after electroweak symmetry breaking. This may reduce the number of relevant parameters and unconstrained combinations in a given measurement. Independent combinations are defined and referred to as *degrees of freedom* from now on. Normalizations and notations are fixed. We recommend to provide experimental and theoretical results in terms of those parameters in the future. We refrain from stating which degrees of freedom are relevant for which process as such a statement is observable dependent. Different factorization schemes (four- or five-flavour) and approximations (e.g., about the CKM matrix, light fermion masses and Yukawa couplings, or subleading electroweak contributions) would impact numerical results. We recommend to determine systematically the dependence of each observable of interest on the listed degrees of freedom. Some illustrative dependences are provided in [Appendix B.3](#) for total rates. More sophisticated observables may be sensitive to additional degrees of freedom or have enhanced dependences on particular combinations.
5. As a starting point, we rely on a tree-level description, working at zeroth order in the loop expansion. All tree-level contributions are considered on an equal footing. Hierarchies between them are only derived from the available experimental constraints. The dependence of a specific observable on a given EFT parameter is possibly omitted only if other measurements constrain that parameter much below the level of sensitivity of this observable. As a result, the inclusion of its dependence should affect neither the pre-existing constraints on that parameter, nor the resulting constraints on others, in a combination of this new measurement with existing ones. This approach is very phenomenological and agnostic about specific theories. In practice, as further and further constraints are collected and combined, a picture will progressively emerge of what specific measurement is particularly relevant to constrain a given direction in parameter space.

The higher-order dependences of observables on SM couplings will be considered in a second step. They could either induce corrections to existing tree-level contributions, or generate a dependence on new EFT parameters. A discussion of next-to-leading order QCD effects on EFT predictions is planned. A variety of results is already available in the literature [6–13].

3 Operator definitions

The definitions of the operators that will be relevant to our discussion —those which contain a top quark for a suitable flavour assignment— are collected here. The associated degrees of freedom, following the flavour assumptions detailed in [Section 4](#), will be defined in [Appendix C](#) and used in the rest of this note. The notation employed in this section is that of Ref. [1] with flavour indices labelled by $ijkl$; left-handed fermion doublets denoted by q, l ; right-handed fermion singlets by u, d, e ; the Higgs doublet by φ ; the antisymmetric $SU(2)$ tensor by $\varepsilon \equiv i\tau^2$; $\tilde{\varphi} = \varepsilon\varphi^*$;

$(\varphi^\dagger \overleftrightarrow{D}_\mu \varphi) \equiv \varphi^\dagger (iD_\mu \varphi) - (iD_\mu \varphi^\dagger) \varphi$; $(\varphi^\dagger \overleftrightarrow{D}_\mu^I \varphi) \equiv \varphi^\dagger \tau^I (iD_\mu \varphi) - (iD_\mu \varphi^\dagger) \tau^I \varphi$ where τ^I are the Pauli matrices; $T^A \equiv \lambda^A/2$ where λ^A are Gell-Mann matrices.

Four-quark operators:

$$O_{qq}^{1(ijkl)} = (\bar{q}_i \gamma^\mu q_j) (\bar{q}_k \gamma_\mu q_l), \quad (1)$$

$$O_{qq}^{3(ijkl)} = (\bar{q}_i \gamma^\mu \tau^I q_j) (\bar{q}_k \gamma_\mu \tau^I q_l), \quad (2)$$

$$O_{qu}^{1(ijkl)} = (\bar{q}_i \gamma^\mu q_j) (\bar{u}_k \gamma_\mu u_l), \quad (3)$$

$$O_{qu}^{8(ijkl)} = (\bar{q}_i \gamma^\mu T^A q_j) (\bar{u}_k \gamma_\mu T^A u_l), \quad (4)$$

$$O_{qd}^{1(ijkl)} = (\bar{q}_i \gamma^\mu q_j) (\bar{d}_k \gamma_\mu d_l), \quad (5)$$

$$O_{qd}^{8(ijkl)} = (\bar{q}_i \gamma^\mu T^A q_j) (\bar{d}_k \gamma_\mu T^A d_l), \quad (6)$$

$$O_{uu}^{(ijkl)} = (\bar{u}_i \gamma^\mu u_j) (\bar{u}_k \gamma_\mu u_l), \quad (7)$$

$$O_{ud}^{1(ijkl)} = (\bar{u}_i \gamma^\mu u_j) (\bar{d}_k \gamma_\mu d_l), \quad (8)$$

$$O_{ud}^{8(ijkl)} = (\bar{u}_i \gamma^\mu T^A u_j) (\bar{d}_k \gamma_\mu T^A d_l), \quad (9)$$

$$\dagger O_{quqd}^{1(ijkl)} = (\bar{q}_i u_j) \varepsilon (\bar{q}_k d_l), \quad (10)$$

$$\dagger O_{quqd}^{8(ijkl)} = (\bar{q}_i T^A u_j) \varepsilon (\bar{q}_k T^A d_l), \quad (11)$$

Two-quark operators:

$$\dagger O_{u\varphi}^{(ij)} = \bar{q}_i u_j \tilde{\varphi} (\varphi^\dagger \varphi), \quad (12)$$

$$O_{\varphi q}^{1(ij)} = (\varphi^\dagger \overleftrightarrow{D}_\mu \varphi) (\bar{q}_i \gamma^\mu q_j), \quad (13)$$

$$O_{\varphi q}^{3(ij)} = (\varphi^\dagger \overleftrightarrow{D}_\mu^I \varphi) (\bar{q}_i \gamma^\mu \tau^I q_j), \quad (14)$$

$$O_{\varphi u}^{(ij)} = (\varphi^\dagger \overleftrightarrow{D}_\mu \varphi) (\bar{u}_i \gamma^\mu u_j), \quad (15)$$

$$\dagger O_{\varphi ud}^{(ij)} = (\tilde{\varphi}^\dagger iD_\mu \varphi) (\bar{u}_i \gamma^\mu d_j), \quad (16)$$

$$\dagger O_{uW}^{(ij)} = (\bar{q}_i \sigma^{\mu\nu} \tau^I u_j) \tilde{\varphi} W_{\mu\nu}^I, \quad (17)$$

$$\dagger O_{dW}^{(ij)} = (\bar{q}_i \sigma^{\mu\nu} \tau^I d_j) \varphi W_{\mu\nu}^I, \quad (18)$$

$$\dagger O_{uB}^{(ij)} = (\bar{q}_i \sigma^{\mu\nu} u_j) \tilde{\varphi} B_{\mu\nu}, \quad (19)$$

$$\dagger O_{uG}^{(ij)} = (\bar{q}_i \sigma^{\mu\nu} T^A u_j) \tilde{\varphi} G_{\mu\nu}^A, \quad (20)$$

Two-quark-two-lepton operators:

$$O_{lq}^{1(ijkl)} = (\bar{l}_i \gamma^\mu l_j) (\bar{q}_k \gamma_\mu q_l), \quad (21)$$

$$O_{lq}^{3(ijkl)} = (\bar{l}_i \gamma^\mu \tau^I l_j) (\bar{q}_k \gamma_\mu \tau^I q_l), \quad (22)$$

$$O_{lu}^{(ijkl)} = (\bar{l}_i \gamma^\mu l_j) (\bar{u}_k \gamma_\mu u_l), \quad (23)$$

$$O_{eq}^{(ijkl)} = (\bar{e}_i \gamma^\mu e_j) (\bar{q}_k \gamma_\mu q_l), \quad (24)$$

$$O_{eu}^{(ijkl)} = (\bar{e}_i \gamma^\mu e_j) (\bar{u}_k \gamma_\mu u_l), \quad (25)$$

$$\dagger O_{lequ}^{1(ijkl)} = (\bar{l}_i e_j) \varepsilon (\bar{q}_k u_l), \quad (26)$$

$$\dagger O_{lequ}^{3(ijkl)} = (\bar{l}_i \sigma^{\mu\nu} e_j) \varepsilon (\bar{q}_k \sigma_{\mu\nu} u_l), \quad (27)$$

$$\dagger O_{ledq}^{(ijkl)} = (\bar{l}_i e_j) (\bar{d}_k q_l), \quad (28)$$

Baryon- and lepton-number-violating operators:¹

$$\dagger O_{duq}^{(ijkl)} = (\bar{d}^c_{i\alpha} u_{j\beta}) (\bar{q}^c_{k\gamma} \varepsilon l_l) \varepsilon^{\alpha\beta\gamma}, \quad (29)$$

$$\dagger O_{quq}^{(ijkl)} = (\bar{q}^c_{i\alpha} \varepsilon q_{j\beta}) (\bar{u}^c_{k\gamma} \varepsilon l_l) \varepsilon^{\alpha\beta\gamma}, \quad (30)$$

¹In the latest version of Ref. [1], $O_{qqq}^{1,3}$ are merged into one single operator with $SU(2)_L$ indices mixed between the two fermion bilinears. The two conventions are technically speaking equivalent [14].

$$\ddagger O_{qqq}^{1(ijkl)} = (\bar{q}_{i\alpha}^c \varepsilon q_{j\beta}) (\bar{q}_{k\gamma}^c \varepsilon l_l) \epsilon^{\alpha\beta\gamma}, \quad (31)$$

$$\ddagger O_{qqq}^{3(ijkl)} = (\bar{q}_{i\alpha}^c \tau^I \varepsilon q_{j\beta}) (\bar{q}_{k\gamma}^c \tau^I \varepsilon l_l) \epsilon^{\alpha\beta\gamma}, \quad (32)$$

$$\ddagger O_{duu}^{(ijkl)} = (\bar{d}_{i\alpha}^c u_{j\beta}) (\bar{u}_{k\gamma}^c e_l) \epsilon^{\alpha\beta\gamma}, \quad (33)$$

Non-Hermitian operators are marked with a double dagger (only in the above list): $\ddagger O$. For Hermitian operators which involve vector Lorentz bilinears, complex conjugation is equivalent to the transposition of generation indices: $O^{(ij)*} = O^{(ji)}$ and by extension, for four-fermion operators, $O^{(ijkl)*} = O^{(jilk)}$. The corresponding effective Lagrangian then takes the form:

$$\mathcal{L} = \sum_a \left(\frac{C_a}{\Lambda^2} \ddagger O_a + \text{h.c.} \right) + \sum_b \frac{C_b}{\Lambda^2} O_b, \quad (34)$$

where the conjugates of the Hermitian operators, labelled here with an index b , are not added. Conventionally and unless otherwise specified, the arbitrary scale Λ will be set to 1 TeV. Equivalently, one could consider that numerical values quoted are in units of TeV^{-2} for the dimensionful coefficients $\tilde{C}_i \equiv C_i/\Lambda^2$. It is understood that the implicit sum over flavour indices only includes independent combinations, i.e., the symmetry in flavour space of the operator coefficients is taken into account.

4 Flavour assumptions

As mentioned in the introduction, prioritizing the study of certain flavour structures is required among the otherwise overwhelming number of four-quark operators. In the lepton sector, it seems manageable to only assume flavour diagonality, i.e. $[U(1)_{l+e}]^3$ which includes a separate $U(1)_l \times U(1)_e$ diagonal subgroup for each of the three lepton generations. This leaves independent parameters for each lepton-antilepton pair of a given generation. This assumption adopted as baseline could, for instance, easily be further restricted to $[U(1)_l \times U(1)_e]^3$, $U(3)_{l+e}$ or even $U(3)_l \times U(3)_e$. As in the quark sector (see below), the third generation of leptons could also be put aside and $U(2)$ symmetries assumed among the first two generations. We discuss different flavour assumptions for the quark sector in the next three sections, starting with a baseline symmetry (Section 4.1) subsequently made less and more restrictive (Sections 4.2 and 4.3).

4.1 Baseline $U(2)_q \times U(2)_u \times U(2)_d$ scenario

As a baseline flavour scenario in the quark sector and motivated —as detailed below— by the minimal flavour violation (MFV) ansatz [15–17], we impose a $U(2)_q \times U(2)_u \times U(2)_d$ symmetry among the first two generations. The MFV expansion of quark bilinear coefficients is the following:

$$\bar{q}_i q_j : a_1 \mathbb{1} + a_2 Y_u Y_u^\dagger + a_3 Y_d Y_d^\dagger + \dots \quad (35)$$

$$\bar{u}_i u_j : b_1 \mathbb{1} + b_2 Y_u^\dagger Y_u + \dots \quad (36)$$

$$\bar{d}_i d_j : c_1 \mathbb{1} + c_2 Y_d^\dagger Y_d + \dots \quad (37)$$

$$\bar{u}_i d_j : d_1 Y_u^\dagger Y_d + \dots \quad (38)$$

$$\bar{q}_i u_j : e_1 Y_u + e_2 Y_u Y_u^\dagger Y_u + e_3 Y_d Y_d^\dagger Y_u + \dots \quad (39)$$

$$\bar{q}_i d_j : f_1 Y_d + f_2 Y_d Y_d^\dagger Y_d + f_3 Y_u Y_u^\dagger Y_d + \dots \quad (40)$$

where a_1, b_1 , etc. are order-one coefficients (see Ref. [18] for the resummation of large contributions in such series). As a first approximation, we assume a unit CKM matrix, and retain only the top and bottom Yukawa couplings, so that $Y_u = \text{diag}(0, 0, y_t)$ and $Y_d = \text{diag}(0, 0, y_b)$. When considering low-energy constraints and restoring the full CKM matrix, one would need to worry about whether UV flavour structures are aligned with the up-, down-quark sectors, or in between

those limits [19]. Denoting the left-handed quark doublet and right-handed quark singlets of the third generation as Q , t , and b ,

$$\begin{aligned} \bar{q}_i q_i, \bar{u}_i u_i, \bar{d}_i d_i & \text{ bilinears are allowed in the first two generations,} \\ \bar{Q}Q, \bar{t}t, \bar{b}b, \bar{t}b, \bar{Q}t, \bar{Q}b & \text{ bilinears are allowed in the third generation,} \end{aligned}$$

under the above assumptions. The coefficients of the first-generation bilinears do not depend on the $i \in \{1, 2\}$ index which is thus implicitly summed over. Fierz transformations may be required on four-fermion operators to bring such quark-antiquark pairs in the same Lorentz bilinear. Equivalently, a $U(2)_q \times U(2)_u \times U(2)_d$ symmetry is assumed between the first two quark generations and no restriction is imposed on the third-generation bilinears. This assumption simplifies four-fermion operators but does not affect third-generation two-fermion ones. Compared to flavour diagonality, i.e. $[U(1)_{q+u+d}]^3$, which would just force quarks and antiquarks to appear in same-flavour pairs, $U(2)_q \times U(2)_u \times U(2)_d$ effectively imposes the following additional requirements:

1. the right-handed charged currents of the first generations ($\bar{u}d, \bar{d}u$) are forbidden,
2. the chirality-flipping bilinears of the first generations ($\bar{q}u, \bar{q}d$) are forbidden,
3. the coefficients of the bilinears of the first and second generations are forced to be identical.

The $U(2)_q \times U(2)_u \times U(2)_d$ flavour symmetry assumption is used by default in this note where not otherwise specified. The following numbers of degrees of freedom are produced for the operators of each category of field content:

four heavy quarks	11 + 2 CPV
two light and two heavy quarks	14
two heavy quarks and bosons	9 + 6 CPV
two heavy quarks and two leptons	(8 + 3 CPV) \times 3 lepton flavours

where we counted separately CP-conserving and CP-violating (CPV) parameters. They are constructed explicitly in [Appendix C](#) and listed in [Table 1](#) together with their definitions in terms of Warsaw-basis operator coefficients.

Finally, a more restrictive variant of this $U(2)_q \times U(2)_u \times U(2)_d$ scenario would retain only the four-fermion operators and exclude the operators with two heavy quarks and bosons. This would be justified when heavy bosons only couple to the SM fermions, so that the low-energy effects are dominated by the tree-level exchanges of heavy mediators between fermionic currents.

4.2 Less restrictive $U(2)_{q+u+d}$ scenario

In order to allow for the light-quark bilinears listed in [item 1](#) and [item 2](#) above, one can limit the flavour symmetry imposed to $U(2)_{q+u+d}$ only, the diagonal subgroup of $U(2)_q \times U(2)_u \times U(2)_d$. The additional 10 + 10 CPV degrees of freedom that then appear for operators containing two light and two heavy quarks are discussed in [Appendix D](#).

4.3 More restrictive *top-philic* scenario

A more restrictive *top-philic* scenario is not obtained by imposing a specific flavour symmetry but rather by assuming that new physics couples dominantly to the left-handed doublet and right-handed up-type quark singlet of the third generation as well as to bosons. All possible operators with this field content are thus constructed. Purely bosonic operators which lead to flavour-universal effects are discarded. A projection onto the Warsaw basis is subsequently performed, notably by employing the equations of motion to trade operators with more derivatives for operators with more fields. In this process, the CKM matrix is again approximated by a unit matrix and all Yukawa couplings but the top and bottom ones are neglected. Only a limited number of

independent Lorentz and colour structures are generated. In terms of the degrees of freedom of the baseline scenario, the ones generated in this case are:

$$c_{t\varphi}^{[I]}, \quad c_{\varphi q}^-, \quad c_{\varphi q}^3, \quad c_{\varphi t}, \quad c_{tW}^{[I]}, \quad c_{tB}^{[I]}, \quad c_{tG}^{[I]}, \quad (41)$$

$$c_{\varphi tb}^{[I]} \quad \text{and} \quad c_{bW}^{[I]} \quad \text{appear proportional to } y_b \quad (42)$$

$$c_{QQ}^1, \quad c_{QQ}^8, \quad c_{Qt}^1, \quad c_{Qt}^8, \quad c_{tt}^1, \quad (43)$$

$$c_{QDW} = c_{Qq}^{3,1} = c_{Ql}^{3(\ell)}, \quad (44)$$

$$c_{QDB} = 6c_{Qq}^{1,1} = \frac{3}{2}c_{Qu}^1 = -3c_{Qd}^1 = -3c_{Qb}^1 = -2c_{Qt}^{1(\ell)} = -c_{Qe}^{(\ell)}, \quad (45)$$

$$c_{tDB} = 6c_{tq}^1 = \frac{3}{2}c_{tu}^1 = -3c_{td}^1 = -3c_{tb}^1 = -2c_{tl}^{(\ell)} = -c_{te}^{(\ell)}, \quad (46)$$

$$c_{QDG} = c_{Qq}^8 = c_{Qu}^8 = c_{Qd}^8 = c_{Qb}^8, \quad (47)$$

$$c_{tDG} = c_{tq}^8 = c_{tu}^8 = c_{td}^8 = c_{tb}^8. \quad (48)$$

All other degrees of freedom then vanish. Counting the degrees of freedom in this scenario, distinguishing operator categories by their field content, one obtains:

$$\begin{array}{ll} \text{two heavy quarks and bosons} & 9 + 6 \text{ CPV} \\ \text{four heavy quarks} & 5 \\ \text{four fermions} & 5. \end{array}$$

5 Example of EFT analysis strategy

An example of analysis strategy is sketched in this section to illustrate how the challenges of global EFT interpretations could be addressed and to highlight what would, in that case, be useful experimental outputs. It relies on fiducial observables defined at, and unfolded to, the particle level.² We stress that other strategies could be equally suitable, more practical to implement in some cases or lead to better sensitivities, by avoiding unfolding. As our aim is illustrative only and as it is in any case difficult to make prescriptions applicable to any type of experimental analysis, we refrain from considering other possibilities in detail. We expect, however, many of the points raised and recommendations made to apply more generally to other analysis strategies. A wealth of EFT analyses has for instance been carried out in the Higgs and electroweak sectors at the LHC and treats issues related to those discussed here (see e.g. Refs. [20–25]).

The approach presented here is meant to be simultaneously practical and useful on a long-term basis. Importantly, it allows for relatively precise reinterpretations without full detector simulation. It could thus easily benefit from future improvements in the accuracy of our EFT predictions and adapt to the evolving picture of global EFT constraints or to changes in underlying assumptions. It should allow to derive robust global constraints and be applicable in a wide variety of situations but could however not lead to the tightest constraints on individual operators. Our rationale is that global constraints have more value than individual ones. A global analysis covers systematically the theory space in direct vicinity of the SM and is able to identify new physics through correlated deviations in precise measurements. A tentative *recipe* could be the following:

1. Define observables at the particle level in a fiducial phase-space volume close enough to the detector level so as to make the unfolding model independent.
 - (a) Several bins of a differential distribution would qualify as examples of observables. A total rate would qualify too, as well as ratios [26, 27], asymmetries, etc.

²A higher level, like the parton one, could be envisioned but would enhance the model-dependence of the unfolding. If advantageous, the *forward folding* of particle-level predictions to the detector level could be considered instead.

- (b) One could also consider observables that are based on multivariate analysis (MVA) techniques. The binned MVA output then yields suitable observables (or, e.g., one bin in several MVA outputs, each maximizing sensitivity to different operator coefficients). The trained classifier(s) should then be provided, for instance as C++ code taking as input a particle-level event sample or kinematic variables.
 - (c) Statistically optimal observables [28–30], similar to matrix element methods (see also Ref. [31, 32]), could be very useful from both theoretical and experimental points of view. Their definitions rely on firm theoretical bases, and encode our physical understanding instead of requiring a resource-intensive and opaque training. They moreover constitute a discrete set exactly sufficient to maximally exploit the available kinematic information on which the effect of higher-order corrections (see e.g. Ref. [33]) or systematic uncertainties can be transparently studied. Applications in experimental analyses include anomalous triple gauge coupling studies at LEP [34–37] and, recently, CP properties of the Higgs boson in di-tau final state [38].
2. Unfold the measurement of these observables, as well as the estimates for the various SM contributions, to the particle level.
 - (a) For a suitably defined fiducial region, the particle and detector levels should be sufficiently close to each other for the unfolding to be performed under the SM hypothesis only. Full simulation at various EFT parameter points would then be avoided altogether. The validity of this approximation should however be checked explicitly.
 - (b) The SM contributions would include both the *signal* and *backgrounds* of a SM measurement. It is important to detail the background composition as these processes could have some EFT dependence which may be neglected at first but which could be desirable to account for at some later point in time.
 3. For the various measurements, provide the statistical and systematics likelihoods, error source breakdown, their correlations, and whether they follow a flat or Gaussian distribution.

Notice that the information above should be sufficient for anybody able to generate an EFT (or any NP) sample at the particle level to set constraints. In order to obtain global EFT constraints, one could further proceed as follows.

4. Compute, numerically or analytically, for each observable O^k , the linear S_i and quadratic S_{ij} contributions of dimension-six operators, in addition to the SM contributions B_l already mentioned in [item 2b](#). Schematically, the expansion in powers of dimension-six operator coefficients can be written as:

$$O^k = B_l^k + \frac{C_i}{\Lambda^2} S_i^k + \frac{C_i C_j}{\Lambda^4} S_{ij}^k + \dots \quad (49)$$

Quadratic and higher powers of dimension-six operator coefficients can be generated at tree level when several operator insertions are possible in one amplitude. The expansion of normalized distributions, ratios, asymmetries, or of the total width appearing in top-quark propagators also generates such higher powers. In some cases, the interference between SM amplitudes and EFT ones could be suppressed (see for instance helicity selection rules discussed in Ref. [39] and references therein) or even vanishingly small (in the case of FCNCs for instance). The dominant contribution could then arise at the quadratic level. Operators of dimension larger than six, in particular that of dimension-eight which were not considered in this note, also start contributing at order $1/\Lambda^4$ in the EFT expansion.

- (a) At tree level, with MG5_aMC@NLO, if a different coupling order EFT_i is given to each of the relevant N operator coefficients C_i , the computation of S_i^k and S_{ij}^k can most easily be done by generating at most $N + N(N + 1)/2$ samples (see [Appendix B](#) for more details, and for the `DIM6_i^2==1` syntax of MG5_aMC@NLO [40] in particular). If

the approximation in [item 2a](#) holds, these samples do not need to be passed through detector simulation.

- (b) As explained in [Section 2](#), it is in principle desirable to include all operators that contribute at some given loop order, say first at the tree level. Exceptions could be made for operators that are much better constrained than the others, at the time at which the limits are extracted. This comparison of the relative strength of different measurements could however evolve with time and the goodness of this approximation be re-evaluated.
5. Within some statistical framework, use the measured O^k , the estimated B_l^k with their statistical and systematic uncertainties, and the S_i^k , S_{ij}^k to derive global constraints on the C_i operator coefficients.
 - (a) It is instructive to also quote individual constraints, set by considering one operator at a time. A comparison between global and individual constraints gives some indication about the magnitude of approximate degeneracies between EFT parameters.
 - (b) For easy combination with other measurements, provide the full covariance matrices of uncertainties on the C_i determination in the Gaussian approximation. The eigenvectors of its inverse corresponding to vanishing eigenvalues indicate which directions of the EFT parameter space remain unconstrained by the measured observables. Other eigenvectors and eigenvalues provide the constraints in other directions.
 - (c) Repeat this procedure twice, with and without including the S_{ij}^k quadratic EFT contributions. The comparison between those two sets of results can explicitly establish where quadratic dimension-six EFT contributions are subleading compared to linear ones. Remarkably, when the linear dependence dominates, the constraints obtained can easily be translated from one basis of dimension-six operators to the other and are therefore of greater generality.
 6. For the purpose of this note, let us define our EFT description to be valid in the regime where it is dominated by dimension-six operator contributions, at the linear level or at some finite higher order. Determining the relative magnitude of the coefficients of operators of various dimensions requires a specific model or power counting. Moreover, the magnitudes of operator-coefficient contributions to a specific observable also depend on E , the characteristic energy scale of the process examined. In a production process at the LHC, the reconstructed partonic centre-of-mass energy is often, theoretically, such a suitable quantity. Other proxies may also be considered like H_T , the scalar sum of all transverse energies. Their correlation with the physically relevant variables should then be studied, as done for instance in [Ref. \[23\]](#) (see [Fig. 2](#) and related discussion). In decays, this characteristic scale E is the mass of the decaying particle.

When it is practically feasible, displaying the variation of the limit as a function of an upper cut on E at E_{cut} (see [Fig. 1](#)) allows for the valid interpretation of EFT results in a larger class of models [\[41, 42\]](#): featuring a new-physics scale lower than the nominal E , or leading to significant contributions from operators of dimension larger than six when no E_{cut} is applied.

Interpreting EFT results in specific models proceeds by expressing each C_i/Λ^2 in terms of the model couplings and mass scales, through a so-called *matching* procedure. The EFT description of a resonance of mass M would be dominated by the operators of lowest dimension when $M \gg E_{\text{cut}}$. Stricter constraints may apply for instance if the resonance has a large width.

7. Besides validity, the quantum perturbativity of the dimension-six EFT can be examined using the same picture. This perturbativity is a necessary condition for the validity (defined as in the previous item) and can be established without reference to a specific model or power counting.

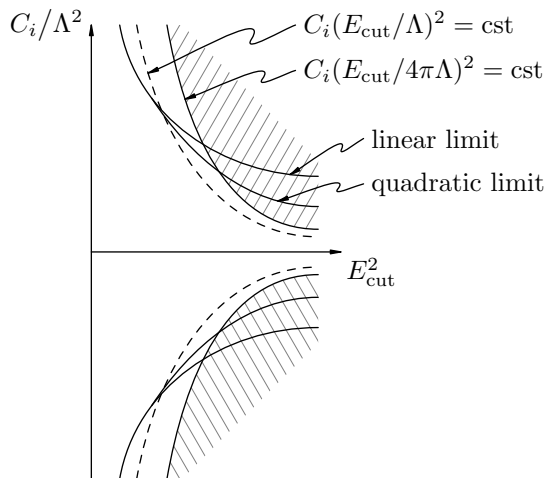


Figure 1: Illustration of the limit set on an EFT parameter as function of a cut on the characteristic energy scale of the process considered (see [item 6](#)). Qualitatively, one expects the limits to be progressively degraded as E_{cut} is pushed towards lower and lower values. At high cut values, beyond the energy directly accessible in the process considered, a plateau should be reached. The regions excluded when the dimension-six EFT is truncated to linear and quadratic orders are delimited by solid lines (see [item 5c](#)). The hatched regions indicate where the dimension-six EFT loses perturbativity (see [item 7](#)). In practice, curves will not be symmetric with respect to $C_i/\Lambda^2 = 0$.

- (a) This quantum perturbativity of the dimension-six EFT is examined through the sum of contributions involving more and more operator insertions in diagrams with higher and higher numbers of loops. The convergence of such a series (involving one additional operator insertion per loop) requires that $C_i(E_{\text{cut}}/4\pi\Lambda)^2$ be smaller than a constant which would roughly be of order one if the normalization of C_i is *natural* to the observable considered. The exact condition would need to be determined on a case-by-case basis. It defines a hyperbola in the $(C_i/\Lambda^2, E_{\text{cut}}^2)$ plane. At tree level, all allowed powers of C_i/Λ^2 can moreover become relevant as soon as $C_i(E_{\text{cut}}/\Lambda)^2$ approaches a constant, possibly of order one. If contributions from higher dimensional operators at the same order in $1/\Lambda$ had similar magnitudes, they would also become relevant at that point.
- (b) If it exists, the point at which the perturbativity hyperbola crosses the limit curves establishes a minimal E_{cut} that has to be imposed for the limit computed perturbatively to make sense. For a sufficiently tight constraint, the limit curves would only cross the perturbativity hyperbola for a cut value beyond the maximal energy directly accessible in the process considered.
- (c) If it exists, the point at which the $C_i(E_{\text{cut}}/\Lambda)^2 = \text{constant}$ hyperbola crosses the limit curve provides a sense of where higher-order terms in the tree-level expansion in powers of dimension-six operator coefficients could become relevant. In particular, one may expect the linear and quadratic limits to start diverging around that point.
- (d) When discussing the relevance of higher-order contributions, definite statements are difficult to make, as is always the case when trying to estimate the terms not computed in a truncated series. As mentioned in [item 4](#), it is worth bearing in mind the first term could for instance have an accidental suppression as it generally arises from the interference of a SM amplitude with an EFT one.

6 Summary and outlook

In this note, we established the first bases of a framework for the EFT interpretation of top-quark measurements at the LHC. Experimental collaborations and theorists are encouraged to use this common language in future publications to facilitate comparisons and combinations. Having mentioned the caveats associated with those choices, we limited our scope to dimension-six operators of the Warsaw basis which contain a top quark, prioritized the study of possible flavour structures with consistent flavour scenarios, defined the degrees of freedom relevant in each case, compiled existing indicative constraints on these parameters, discussed the use of simulation tools to extract their dependence, and tabulated several benchmark results. An example of analysis strategy

was also sketched to illustrate one possible way in which the challenges of a global EFT analysis could be addressed. The experimental outputs that are in that case desirable were highlighted. It is expected that the statements made in the discussion of this example could be transposed to concrete analyses and adapted to different strategies.

Having laid those bases, we did not address more involved issues like next-to-leading order corrections (especially in QCD), theoretical uncertainties, or the treatment of unstable tops. These important topics may deserve further discussion in the LHC TOP Working Group. It is left to the communities of both theorists and experimentalists to study the observables that are best suited to constrain particular direction of the EFT parameter space and to examine the complementarity between them as well as between different processes. Combining the constraints from various sources or determining which dependences are relevant in each observable are tasks that should also be addressed to make progress in the program outlined here. Ultimately, it will be important to combine top-quark, Higgs and electroweak measurements within the SMEFT. Studies targeting these two other sectors are discussed in the corresponding LHC HXS and EW Working Groups. Several methodological points raised in this note, such as those discussed in [Section 5](#), have also been addressed in these contexts, see for example Ref. [\[43\]](#).

Finally, as stressed several times in this note, the global EFT picture will necessarily evolve with time as new measurements and more accurate predictions become available. Some of the assumptions made here may therefore need to be revised in the future as a finer picture is obtained.

Acknowledgements

We would like to warmly thank the experimentalists of the ATLAS and CMS Collaborations having provided us with extensive feedback on the content of this note, the participants to the LHC TOP Working Group meetings in which it was discussed, and the conveners of the Working Group for their support.

A Indicative constraints

As a reference, we collect here various limits set by theoretical studies on the relevant degrees of freedom. We note that there is presently no study considering all the operators listed above and therefore no marginalised constraints are available. Typically, the fits considering one operator at a time (or marginalising over a smaller subset of operators) provide more stringent constraints. The limits listed should therefore only serve as a guidance for potential sensitivity studies or fits. Direct limits arising from the top-quark measurements are given in [Table 1](#), where available. Indirect limits from low-energy observables also exist, some of which can be very strong yet more model dependent. Limits from B decays, dilepton production, electroweak precision observables, as well as electric dipole moments and CP asymmetries are discussed in the following three subsections.

A.1 Constraints from low-energy flavour physics

The CKM matrix can be approximated as the identity matrix when focusing on measurements involving resonant top quarks. However, when confronting new physics models with flavour observables, suppressed in the SM by small CKM matrix elements, it is of course crucial to consistently keep all the CKM factors. By working in the down-quark mass basis, the misalignment between the up- and down- quark masses can be described by considering the quark doublet as $q_i = (V_{ji}^* u_{L,j}, d_{L,i})^T$. Another basis often used is the one where up quarks have diagonal mass matrix. This can be obtained by simply rotating q_i with the CKM matrix: $\tilde{q}_i = (Vq)_i = (u_{L,i}, V_{ij} d_{L,j})^T$. This choice changes the flavour structure of the operators by the same CKM rotations, for example the term $C^{(ij)} \bar{q}_i \gamma_\mu q_j \rightarrow \tilde{C}^{(ij)} \bar{\tilde{q}}_i \gamma_\mu \tilde{q}_j$, where $\tilde{C} = V C V^\dagger$. In the spirit of this note, we assume that the (33) element of such flavour matrices is the largest one. The $U(2)_q$ flavour symmetry relates the off-diagonal components to the CKM matrix [\[48, 49\]](#). In this well motivated framework, in general the new physics contributions are not necessarily aligned

Four-heavy (11 + 2 CPV d.o.f.)	Indicative direct limits
$c_{QQ}^1 \equiv 2C_{qq}^{1(3333)} - \frac{2}{3}C_{qq}^{3(3333)}$	
$c_{QQ}^8 \equiv 8C_{qq}^{3(3333)}$	
$!c_{QQ}^+ \equiv C_{qq}^{1(3333)} + C_{qq}^{3(3333)}$	$[-2.92, 2.80] (E_{cut} = 3 \text{ TeV})$ [44]
$c_{Qt}^1 \equiv C_{qu}^{1(3333)}$	$[-4.97, 4.90] (E_{cut} = 3 \text{ TeV})$ [44]
$c_{Qt}^8 \equiv C_{qu}^{8(3333)}$	$[-10.3, 9.33] (E_{cut} = 3 \text{ TeV})$ [44]
$c_{Qb}^1 \equiv C_{qd}^{1(3333)}$	
$c_{Qb}^8 \equiv C_{qd}^{8(3333)}$	
$c_{tt}^1 \equiv C_{uu}^{(3333)}$	$[-2.92, 2.80] (E_{cut} = 3 \text{ TeV})$ [44]
$c_{tb}^1 \equiv C_{ud}^{1(3333)}$	
$c_{tb}^8 \equiv C_{ud}^{8(3333)}$	
$c_{QtQb}^{1[I]} \equiv \frac{[\text{Im}]\{C_{quqd}^{1(3333)}\}}{\text{Re}}$	
$c_{QtQb}^{8[I]} \equiv \frac{[\text{Im}]\{C_{quqd}^{8(3333)}\}}{\text{Re}}$	
Two-light-two-heavy (14 d.o.f.)	
$c_{Qq}^{3,1} \equiv C_{qq}^{3(ii33)} + \frac{1}{6}(C_{qq}^{1(i33i)} - C_{qq}^{3(i33i)})$	$[-0.66, 1.24]$ [45], $[-3.11, 3.10]$ [44]
$c_{Qq}^{3,8} \equiv C_{qq}^{1(i33i)} - C_{qq}^{3(i33i)}$	$[-6.06, 6.73]$ [44]
$c_{Qq}^{1,1} \equiv C_{qq}^{1(ii33)} + \frac{1}{6}C_{qq}^{1(i33i)} + \frac{1}{2}C_{qq}^{3(i33i)}$	$[-3.13, 3.15]$ [44]
$c_{Qq}^{1,8} \equiv C_{qq}^{1(i33i)} + 3C_{qq}^{3(i33i)}$	$[-6.92, 4.93]$ [44]
$c_{Qu}^1 \equiv C_{qu}^{1(33ii)}$	$[-3.31, 3.44]$ [44]
$c_{Qu}^8 \equiv C_{qu}^{8(33ii)}$	$[-8.13, 4.05]$ [44]
$c_{Qd}^1 \equiv C_{qd}^{1(33ii)}$	$[-4.98, 5.02]$ [44]
$c_{Qd}^8 \equiv C_{qd}^{8(33ii)}$	$[-11.7, 9.39]$ [44]
$c_{tq}^1 \equiv C_{qu}^{1(ii33)}$	$[-2.84, 2.84]$ [44]
$c_{tq}^8 \equiv C_{qu}^{8(ii33)}$	$[-6.80, 3.49]$ [44]
$c_{tu}^1 \equiv C_{uu}^{(ii33)} + \frac{1}{3}C_{uu}^{(i33i)}$	$[-3.62, 3.57]$ [44]
$c_{tu}^8 \equiv 2C_{uu}^{(i33i)}$	$[-8.05, 4.75]$ [44]
$c_{td}^1 \equiv C_{ud}^{1(33ii)}$	$[-4.95, 5.04]$ [44]
$c_{td}^8 \equiv C_{ud}^{8(33ii)}$	$[-11.8, 9.31]$ [44]
Two-heavy (9 + 6 CPV d.o.f.)	
$c_{t\varphi}^{[I]} \equiv \frac{[\text{Im}]\{C_{u\varphi}^{(33)}\}}{\text{Re}}$	
$c_{\varphi q}^- \equiv C_{\varphi q}^{1(33)} - C_{\varphi q}^{3(33)}$	$c_{\varphi q}^1$ $[-3.1, 3.1]$ [45], $[-8.3, 8.6]$ [46]
$c_{\varphi Q}^3 \equiv C_{\varphi q}^{3(33)}$	$[-4.1, 2.0]$ [45], $[-8.6, 8.3]$ [46]
$c_{\varphi t} \equiv C_{\varphi u}^{(33)}$	$[-9.7, 8.3]$ [45], $[-9.1, 9.1]$ [46]
$c_{\varphi tb}^{[I]} \equiv \frac{[\text{Im}]\{C_{\varphi ud}^{(33)}\}}{\text{Re}}$	
$c_{tW}^{[I]} \equiv \frac{[\text{Im}]\{C_{uW}^{(33)}\}}{\text{Re}}$	c_{tW} $[-4.0, 3.5]$ [45], $[-4.1, 4.1]$ [46]
$c_{tZ}^{[I]} \equiv \frac{[\text{Im}]\{-s_W C_{uB}^{(33)} + c_W C_{uW}^{(33)}\}}{\text{Re}}$	c_{tB} $[-6.9, 4.6]$ [45], $[-7.6, 7.6]$ [46]
$c_{bW}^{[I]} \equiv \frac{[\text{Im}]\{C_{dW}^{(33)}\}}{\text{Re}}$	
$c_{tG}^{[I]} \equiv \frac{[\text{Im}]\{C_{uG}^{(33)}\}}{\text{Re}}$	c_{tG} $[-1.32, 1.24]$ [45]
Two-heavy-two-lepton (8 + 3 CPV d.o.f. $\times 3$ lepton flavours)	
$c_{Ql}^{3(\ell)} \equiv C_{lq}^{3(\ell\ell33)}$	
$c_{Ql}^{-1(\ell)} \equiv C_{lq}^{1(\ell\ell33)} - C_{lq}^{3(\ell\ell33)}$	
$c_{Qe}^{(\ell)} \equiv C_{eq}^{(\ell\ell33)}$	
$c_{tl}^{(\ell)} \equiv C_{lu}^{(\ell\ell33)}$	
$c_{te}^{(\ell)} \equiv C_{eu}^{(\ell\ell33)}$	
$c_t^{S[I](\ell)} \equiv \frac{[\text{Im}]\{C_{lequ}^{1(\ell\ell33)}\}}{\text{Re}}$	
$c_t^{T[I](\ell)} \equiv \frac{[\text{Im}]\{C_{lequ}^{3(\ell\ell33)}\}}{\text{Re}}$	
$c_b^{S[I](\ell)} \equiv \frac{[\text{Im}]\{C_{ledq}^{(\ell\ell33)}\}}{\text{Re}}$	

Table 1: Indicative limits on top-quark operator coefficients for $\Lambda = 1 \text{ TeV}$. For details on the fit procedure, information on the input data and set of operators over which the results are marginalised please consult the corresponding references (see also Ref. [47]). Coefficients marked with a ‘!’ are not independent of the ones previously defined.

with the up or down quarks, but will have some misalignment of the order of the relevant CKM elements. For definiteness, in the following we mostly work in the down-quark mass basis.

Let us consider the charged-current transition $b \rightarrow c e_i \bar{\nu}_j$ and study the experimental limits we can extract on the top-quark operators. From the general effective Hamiltonian at the B -meson mass scale, we can consider only the operators involving the left-handed c_L quark, since c_R necessarily arises from a second-generation family index. We are left with

$$H_{\text{eff}}^{b \rightarrow ce\bar{\nu}} = -\frac{2}{v^2} V_{cb} \left((\delta^{ij} + c_{V_L}^{ij}) (\bar{c}_L \gamma^\mu b_L) (\bar{e}_L^i \gamma_\mu \nu_L^j) + c_{S_R}^{ij} (\bar{c}_L b_R) (\bar{e}_R^i \nu_L^j) + h.c. \right), \quad (50)$$

where $v \approx 246$ GeV. The tree-level matching to the SMEFT is given by [50, 51]

$$\begin{aligned} c_{V_L}^{ij} &= -\frac{v^2}{\Lambda^2} \left(\frac{\sum_k V_{ck} C_{lq}^{3(ijk3)}}{V_{cb}} \right) + \frac{v^2}{\Lambda^2} \left(\frac{\sum_k V_{ck} C_{\varphi q}^{3(k3)}}{V_{cb}} \right) \delta^{ij}, \\ c_{S_R}^{ij} &= -\frac{v^2}{\Lambda^2} \frac{\sum_k V_{ck} C_{ledq}^{(ji3k)}}{V_{cb}}, \end{aligned} \quad (51)$$

where $k = 1, 2, 3$ and for simplicity we assumed real coefficients. In general, under the $U(2)_q$ symmetry, the contribution from the (33) element and from the (23) one are of the same order since, for example $C_{lq}^{3(ij23)}/C_{lq}^{3(ij33)} \sim \mathcal{O}(V_{cb})$. In realistic fits to these observables it is thus important to keep track of all contributions, which can lead to important phenomenological consequences (see e.g. Ref. [52]). Nevertheless, in order to extract the indicative numerical constraints, in the following we assume *down-alignment* and keep as non vanishing only the (33) element of these operators.

Consistently with the rest of the note, we neglect lepton-flavour-violating terms, while we allow possible deviations from lepton-flavour universality. In the case of operators with electron and muon one can derive the constraints from $B \rightarrow D^{(*)} \ell \nu$ decays [53], which experimentally agree with the SM prediction. In the case of the τ lepton, instead, the corresponding decays $B \rightarrow D^{(*)} \tau \nu$ show an interesting deviation from the SM prediction with a statistical significance of more than 4σ [54–58]. In particular, the relevant observables are ratios between the decay modes to tau and light leptons in which hadronic uncertainties largely cancel. Combining the different measurements one can express the result as (see e.g. Ref. [52])

$$R_{D^{(*)}} \equiv \frac{\mathcal{B}(B \rightarrow D^{(*)} \tau \nu)}{\mathcal{B}(B \rightarrow D^{(*)} \ell \nu)} \left(\frac{\mathcal{B}(B \rightarrow D^{(*)} \tau \nu)_{\text{SM}}}{\mathcal{B}(B \rightarrow D^{(*)} \ell \nu)_{\text{SM}}} \right)^{-1} = |1 + c_{V_L}^{\tau\tau}|^2 = 1.237 \pm 0.053, \quad (52)$$

where we showed explicitly only the contribution from the vector operator. This corresponds to $c_{V_L}^{\tau\tau} = 0.112 \pm 0.024$. While also the scalar operator $c_{S_R}^{\tau\tau}$ contributes to the observables above, with a different weight in R_D compared to R_{D^*} , a stronger constraint can be derived from the B_c lifetime [59], due to the chiral enhancement of the scalar contribution. This gives an approximate bound $|c_{S_R}^{\tau\tau}| \lesssim 0.39$, which should be compared to the value $c_{S_R} \approx 1.5$ that would be required to fit R_{D^*} . In the case of down-alignment, a non-vanishing contribution to $D - \bar{D}$ mixing is generated by the CKM rotation from the $O_{qq}^{1(3333)}$ and $O_{qq}^{3(3333)}$ operators:

$$\mathcal{L}_{\text{eff}} \supset \frac{C_{qq}^{1(3333)} + C_{qq}^{3(3333)}}{\Lambda^2} (V_{ub} V_{cb}^*)^2 (\bar{u}_L \gamma_\mu c_L)^2 + h.c. . \quad (53)$$

This can be used to cast a limit on the combination above [60]. The limits expressed in terms of the degrees of freedom defined in this note are reported in Table 2.

With the choice of down-alignment, contributions to $b \rightarrow s$ transitions, such as in $B \rightarrow K^{(*)} \ell^+ \ell^-$ decays or in $B_s - \bar{B}_s$ mixing, arise proportionally to the off-diagonal (32) element of the quark flavour matrix of the various operators. While, as already mentioned, the $SU(2)_q$ flavour symmetry predicts that this element should be of $\mathcal{O}(V_{cb})$, in the simplified discussion above this was put to zero by hand, thus forbidding tree-level contributions to these processes. It is worthwhile to

Four-heavy				
c_{QQ}^+	$\equiv C_{qq}^{1(3333)} + C_{qq}^{3(3333)}$	$[-21, 21]$ [60]	(from $D - \bar{D}$, with down-alignment)	
\tilde{c}_{QQ}^+	$\equiv \tilde{C}_{qq}^{1(3333)} + \tilde{C}_{qq}^{3(3333)}$	$[-0.03, 0.03]$ [60]	(from $B_s - \bar{B}_s$, with up-alignment)	
Two-heavy-two-lepton		$\ell = e$	$\ell = \mu$	$\ell = \tau$
$c_{Ql}^{3(\ell)}$	$\equiv C_{lq}^{3(\ell\ell33)}$	$[-0.57, 0.22]$ [53]	$[-0.22, 0.57]$ [53]	-1.85 ± 0.40 [52]
$c_b^{S(\ell)}$	$\equiv \text{Re}\{C_{ledq}^{(\ell\ell33)}\}$	$[-10, 10]$ [53]	$[-17, 13]$ [53]	$[-13, 13]$ [59]

Table 2: Indicative limits on top-quark operators arising from semileptonic B decays and heavy meson oscillations and for $\Lambda = 1$ TeV.

Two-heavy-two-lepton		$\ell = e$	$\ell = \mu$	$\ell = \tau$
$c_{Ql}^{-\ell} + 2c_{Ql}^{3(\ell)}$	$\equiv C_{lq}^{1(\ell\ell33)} + C_{lq}^{3(\ell\ell33)}$	$[-0.32, 0.20]$ [64]	$[-0.43, 0.34]$ [64]	$[-2.6, 2.6]$ [65]
$c_{Qe}^{(\ell)}$	$\equiv C_{eq}^{(\ell\ell33)}$	$[-0.24, 0.28]$ [64]	$[-0.38, 0.40]$ [64]	–
$c_b^{S(\ell)}$	$\equiv \text{Re}\{C_{ledq}^{(\ell\ell33)}\}$	–	–	$[-1.9, 1.9]$ [65]

Table 3: Indicative limits on top-quark operators arising from dilepton pair production at the LHC and with $\Lambda = 1$ TeV.

briefly discuss what would happen in the opposite scenario of *up-alignment*, where the operators are written in terms of $\tilde{q}_i = (u_{L,i}, V_{ij}d_{L,j})^T$ and only the (33) component of the flavour matrix is left non-vanishing. In this case the $b \rightarrow d_i$ transition would arise proportionally to V_{ib} , while there would be no $b \rightarrow c$ charged-current transition (which, in this case, would be strictly proportional to the (32) element of the flavour matrices). $\Delta F = 2$ processes in the down sector, therefore, put strong limits at tree level on four-quark operators:

$$\mathcal{L}_{\text{eff}} \supset \frac{\tilde{C}_{qq}^{1(3333)} + \tilde{C}_{qq}^{3(3333)}}{\Lambda^2} [(V_{ts}V_{tb}^*)^2(\bar{b}_L\gamma_\mu s_L)^2 + (V_{td}V_{tb}^*)^2(\bar{b}_L\gamma_\mu d_L)^2 + (V_{td}V_{ts}^*)^2(\bar{s}_L\gamma_\mu d_L)^2] + h.c. \quad (54)$$

In particular, the strongest constraint on the overall coefficient is from $B_s - \bar{B}_s$ mixing [60]. The measurement of various $b \rightarrow s\ell^+\ell^-$ transitions would instead constrain the two-quark-two-lepton operators $\tilde{O}_{lq}^{1(ij33)}$, $\tilde{O}_{lq}^{3(ij33)}$, and $\tilde{O}_{eq}^{(ij33)}$ (see e.g. Refs. [61, 62]). Loop-level contributions to B_s mixing and electroweak precision measurements can instead be used to put constraints on the $\tilde{O}_{\varphi q}^{1(33)}$, $\tilde{O}_{\varphi q}^{3(33)}$, and $\tilde{O}_{\varphi u}^{(33)}$ operators [63]. It is clear that both up- and down-alignment are very particular cases. Experimentally, since limits from $\Delta F = 2$ processes are stronger in the down sector, the down-alignment case might be preferred. Generic models of flavour are expected to interpolate between the two scenarios, therefore a more general analysis, which is well beyond the purpose of the present note, would be advisable.

A.2 Constraints from high- p_T di-lepton searches

It is well known that the high-energy tail of $2 \rightarrow 2$ scattering processes is very sensitive to effective operators, since it allows to use the growth with energy of the new physics amplitudes to increase the signal over background ratio. In particular, let us focus here on fermion-fermion scattering processes at the LHC such as $q\bar{q} \rightarrow q\bar{q}$ and $q\bar{q} \rightarrow \ell^+\ell^-$. These have been shown to provide very strong constraints on four-fermion operators [50, 64–68]. Since the sensitivity comes from the high energy tail, the issue of the validity of the EFT expansion is a crucial one to be addressed in this case. In particular, the underlying assumption for these bounds to be valid is that the maximal centre of mass energy from which the sensitivity is gained, E_{max} , has to be much smaller than the mass scale of the heavy states which have been integrated out, $E_{\text{max}} \ll M_{\text{NP}}$. This issue has been studied in detail in the references above and it has been shown that there exist models in which the new states are heavy enough for the EFT approach to be valid, and for

which the constraints obtained are relevant. For example, in Ref. [64], it has been shown that $q\bar{q} \rightarrow e^+e^-, \mu^+\mu^-$ processes can be used to put significant constraints on some models addressing the neutral-current B -physics anomalies. Instead, the EFT interpretation of the limits in the $\tau\tau$ final state [65] should be taken as indicative only, since the mass scale of new physics cannot be too high in that case. Nevertheless, comparing with the limits on explicit models [65] shows that the EFT ones still provide a good first-order indication. In Table 3 we report the limits from [64, 65] on the two-quark-two-lepton operators involving third generation quarks, in particular the b quark since it is the only one accessible in the initial state.

A.3 Indirect constraints from electroweak precision observables

Electroweak precision observables (EWPOs) provide additional constraints on the top-quark operators. These measurements include the Z -pole data from LEP and SLC, the fermion pair production and W pair production from LEP2, W mass and width measurements from LEP and Tevatron, and other low-energy measurements such as DIS and atomic parity violation. These measurements do not directly involve resonant top quarks. The constraints come only from the top-quark loop-induced contributions in the two-point functions of the electroweak gauge bosons, which are modified by top-quark operators. Unlike in the SM, these contributions are in general UV divergent, and therefore they need to be interpreted with care. On the one hand, we aim to get as much information as possible, while on the other hand, we would like to base our approach only on minimum set of assumptions, so that the resulting constraints are meaningful for a wide range of BSM scenarios. The approach adopted in Refs. [69, 70] is an example of a reasonable balance between these two aspects.

Consider the following subset of the two-heavy degrees of freedom

$$c_{\varphi Q}^-, c_{\varphi Q}^3, c_{\varphi t}, c_{tW}, c_{tB}, c_{bW} \quad (55)$$

that are relevant in the EWPOs. One specific contribution,

$$c_{\varphi Q}^- + 2c_{\varphi Q}^3, \quad (56)$$

corresponds to $Z \rightarrow b\bar{b}$ and can be constrained at the tree-level. All the other degrees of freedom enter only through the modification of the self-energies of W , Z and γ at the loop level. These contributions consist of two parts:

- (a) the UV poles and the corresponding logarithmic terms,
- (b) the remaining finite terms.

The UV poles in the first part need to be cancelled by the renormalization of the following two non-top operators, to get physical results:

$$O_{\varphi WB} = (\varphi^\dagger \tau^I \varphi) W_{\mu\nu}^I B^{\mu\nu} \quad (57)$$

$$O_{\varphi D} = (\varphi^\dagger D^\mu \varphi)^* (\varphi^\dagger D_\mu \varphi) \quad (58)$$

In other words, the top-quark operators mix into these two operators.³ After the renormalization, contribution (a) gives a linear q^2 -dependent part in all the self-energy functions $\Pi_{VV}(q^2)$. These contributions can be identified as a change of the S and T parameters. It is well known that the EWPOs places stringent bounds on the S and T parameters, and so naively one could apply these bounds to constrain the top-quark operators. However, given that $O_{\varphi WB}$ and $O_{\varphi D}$ are included

³This statement is basis dependent. In this study we use the ‘‘HISZ’’ basis [71], which is convenient for oblique physics effects, but we keep the definitions of $O_{\varphi WB}$ and $O_{\varphi D}$ to be consistent with the Warsaw basis. The physics result is basis-independent. In the Warsaw basis, some of the counter terms for the oblique parameters will be provided by other operators involving fermion fields.

Two-heavy

$c_{\varphi q}^- + 2c_{\varphi Q}^3$	$\equiv C_{\varphi q}^{1(33)} + C_{\varphi q}^{3(33)}$	0.016 ± 0.021
$c_{\varphi q}^-$	$\equiv C_{\varphi q}^{1(33)} - C_{\varphi q}^{3(33)}$	2.0 ± 2.7
$c_{\varphi t}$	$\equiv C_{\varphi u}^{(33)}$	1.8 ± 1.9
c_{tW}	$\equiv \text{Re}\{C_{uW}^{(33)}\}$	-0.4 ± 1.2
c_{tB}	$\equiv \text{Re}\{C_{uB}^{(33)}\}$	4.8 ± 5.3
c_{bW}	$\equiv \text{Re}\{C_{dW}^{(33)}\}$	11 ± 13

Table 4: Indicative limits on top-quark operators arising from precision electroweak observables, with $\Lambda = 1$ TeV.

to obtain physical results, they need to be incorporated in the calculations of S and T . One finds, for example for c_{tW} ,

$$\hat{S} = \frac{c_{\varphi WB}(\mu)v^2}{\Lambda^2} \frac{c_W}{s_W} - N_c \frac{gc_{tW}}{4\pi^2} \frac{\sqrt{2}vm_t}{4\Lambda^2} \frac{5}{3} \ln \frac{m_t^2}{\mu^2} \quad (59)$$

which prevents us from directly setting bounds on c_{tW} , as the value of $c_{\varphi WB}(\mu)$ is unknown. Here μ is the renormalization scale. Indicative bounds may be obtained by assuming “no accidental cancellation” between the two terms, allowing us to set $c_{\varphi WB}(\mu) = 0$. However, since the mixing effect exists, the results strongly depend on the scale μ at which this assumption is made.⁴

Nevertheless, useful information can be obtained from contribution (b). By definition the S and T parameters assume a linear q^2 dependence for all two-point functions $\Pi_{VV}(q^2)$. This is not the case when loop-contributions are the dominant ones, in particular the finite terms in (b) are in general not linear q^2 functions. On the other hand, the EWPOs contain more information than the S and T parameters. To extract this information, one needs to abandon the oblique parameter formalism and perform a global fit for all measurements, including the top-loop contributions in all theory predictions. $c_{\varphi WB}(\mu)$ and $c_{\varphi D}(\mu)$ should be included, to obtain physical predictions. In the resulting χ^2 , one then marginalizes over the $c_{\varphi WB}(\mu)$ and $c_{\varphi D}(\mu)$ coefficients. The remaining constraints become weaker, but they are more reliable as they do not depend on any specific assumptions on these two coefficients. One can also check that the constraints obtained in this way are independent of the renormalization scale μ , to confirm that these results are physical.

The details of this analysis can be found in Ref. [70]. We summarize the results on the relevant degrees of freedom, as indicative constraints in Table 4, assuming only one top operator is considered at a time.⁵

As a final remark, apart from $O_{\varphi WB}$ and $O_{\varphi D}$, one could certainly include more non-top operators and perform a more global EW fit. The results will be more model-independent, at the cost of weakening the limits one would get after marginalizing over the non-top operators. The reason for only incorporating the $O_{\varphi WB}$ and $O_{\varphi D}$ operators here, is that they are the only ones to which the top-quark operators mix, and therefore the minimum set of operators one has to incorporate in order to extract exactly the part (b) contributions, which are μ independent and therefore more physical. This however implies that the resulting limits are based on the assumption that the dominant BSM effects are captured by top-quark operators.

⁴The most constraining bounds obtained in this way corresponds to setting $\mu = \Lambda$ in Eq. (59) and assuming $c_{\varphi WB}(\Lambda) = 0$. This is often called the renormalization-group-induced bounds in the literature. They are however strongly model-dependent as assumptions about the matching scale are required, and are not consistent with the global EFT picture as a bottom-up approach. Therefore we do not discuss these bounds here and refer the interested readers to Refs. [63, 72–74].

⁵Ref. [75] also constrained both $c_{\varphi q}^- + 2c_{\varphi Q}^3$ and $c_{\varphi q}^-$ by combining $e^+e^- \rightarrow Z \rightarrow b\bar{b}$ measurements with single top-quark t -channel production at hadron colliders.

A.4 Indirect constraints from low-energy probes of CP violation

In addition to limits from direct observables, complementary constraints can be derived from low-energy measurements. Such indirect observables do not involve resonant top quarks, but they are affected, in some cases very significantly, by virtual top quarks and as such can be used to probe SMEFT top-quark operators. Here we focus on a subset of SMEFT operators, namely the operators defined in [Appendix C](#) that violate CP, which are mainly constrained by electric-dipole-moment (EDM) experiments and asymmetry measurements in $B \rightarrow X_s \gamma$. Although we do not change the flavour structure of the operators themselves, we will deviate slightly from the baseline flavour assumptions of [Section 4](#). In particular, we restore the off-diagonal CKM matrix elements and the light Yukawa couplings. Although these small SM parameters can be neglected in direct probes, they give rise to loop diagrams that, in some cases, induce the dominant contributions to low-energy probes. Indirect constraints on the CP-even parts, coming from electroweak precision data, are discussed in the next subsection.

As not all readers might be familiar with EDM phenomenology we give a brief introduction here. EDMs of leptons, nucleons, atoms, and molecules are probes of flavour-diagonal CPV that suffer from essentially no SM background. While the CKM mechanism predicts nonzero EDMs, they are orders of magnitude below the current experimental limits. At present, the strongest EDM constraints arise from measurements on three different systems: the neutron, the ^{199}Hg atom, and the polar molecule ThO. The limit on the latter can be interpreted (with care) as a limit on the electron EDM. In order to interpret measurements on these complicated systems in terms of the SMEFT Wilson coefficients, several steps need to be taken. First of all, the SMEFT operators must be evolved to lower energies, typically up to a scale of a few GeV where QCD is still perturbative. At that point, the SMEFT operators are matched to an effective Lagrangian describing the dynamics of the relevant low-energy degrees of freedom such as nucleons, pions, photons, and electrons. This effective Lagrangian is then used to calculate the EDMs of nucleons, nuclei, atoms, and molecules. A detailed discussion is beyond the scope of this note, and below we briefly describe how to connect the limit on the neutron and electron EDM to the SMEFT Wilson coefficients.

We start by discussing the limits from the neutron EDM. This observable obtains contributions from several CPV operators, namely four of the top-Higgs couplings, $c_{t\varphi}$, c_{tG} , c_{bW} , and $c_{\varphi tb}$, as well as the four-quark operator coefficients, $c_{Q_t Q_b}^{1,8}$. To estimate the limits, we evolve these operators, by using renormalization-group equations (RGEs), from the scale of new physics, Λ , to the scale of the top-quark mass. At this scale we integrate out the top quark. Here both $c_{t\varphi}$ and c_{tG} induce a threshold contribution to a purely gluonic CPV operator without top quarks, the so-called Weinberg operator

$$\mathcal{L}_W = \frac{g_S}{6} \frac{d_W}{\Lambda^2} f^{abc} \epsilon^{\mu\nu\alpha\beta} G_{\alpha\beta}^a G_{\mu\rho}^b G_{\nu\rho}^c, \quad (60)$$

with [\[76–81\]](#)

$$d_W(m_t) = \frac{g_S^2}{64\pi^4} \frac{v}{\sqrt{2}m_t} h(m_t, m_h) c_{t\varphi}^I + \frac{g_S^2}{(4\pi)^2} \frac{v}{\sqrt{2}m_t} c_{tG}^I, \quad (61)$$

where $h(m_t, m_h) \simeq 0.05$ is a finite two-loop integral. Note that $c_{t\varphi}^I$ also contributes to the EDMs of light quarks, proportional to their Yukawa couplings, through two-loop Barr-Zee diagrams [\[82–85\]](#). We include this effect in the limits discussed below.

In addition, $c_{\varphi tb}$, c_{bW} , and $c_{Q_t Q_b}^{1,8}$ contribute to the Weinberg operator by first inducing the bottom chromo-EDM, $O_{dG}^{(33)}$. For the four-quark operators and $O_{dW}^{(33)}$ the bottom chromo-EDM is induced through renormalization-group evolution [\[86–88\]](#) between $\mu = \Lambda$ and $\mu = m_t$, while $O_{\varphi tb}$ only provides a matching contribution

$$\frac{d\text{Im } C_{dG}^{(33)}}{d \ln \mu} = \frac{\sqrt{2}}{(4\pi)^2} \frac{m_t}{v} \left(c_{Q_t Q_b}^{1I} - \frac{1}{2N_C} c_{Q_t Q_b}^{8I} \right) + \frac{2}{(4\pi)^2} \left[3g_W^2 + \frac{1}{3}g_Y^2 \right] c_{bW}^I \dots,$$

$$\text{Im } C_{dG}^{(33)}(m_t^-) = \text{Im } C_{dG}^{(33)}(m_t^+) + \frac{1}{\sqrt{2}(4\pi)^2} \frac{m_t}{v} f_W c_{\varphi tb}^I, \quad (62)$$

where $f_W \simeq 0.7$ is a loop function [89] and the ellipsis stands for the self-renormalization. At the bottom mass scale $O_{dG}^{(33)}$ then induces a contribution to the Weinberg operator

$$d_W(m_b^-) = d_W(m_b^+) + \frac{g_S^2}{(4\pi)^2} \frac{v}{\sqrt{2}m_b} \text{Im}(C_{dG}^{(33)}(m_b^+)). \quad (63)$$

The Weinberg operator can now be evolved to lower energies and, around the QCD scale, be matched to hadronic operators. In particular, it induces a contribution to the neutron EDM

$$|d_n| \simeq (50 \text{ MeV}) e g_s (1 \text{ GeV}) d_W(1 \text{ GeV}) / \Lambda^2. \quad (64)$$

The required hadronic matrix element suffers from large uncertainties and here we have taken the average of various estimates [77, 90, 91]. The impact of hadronic and nuclear uncertainties on low-energy precision constraints on the SMEFT operators can be significant and has been discussed in detail in Refs. [88, 92]. The constraints that result from employing Eq. (64) and the experimental limit, $d_n < 3.0 \cdot 10^{-13} \text{ e fm}$ [93, 94], are collected in Table 5.

Moving on to the electron EDM, there are again several operators that contribute, namely, three top-Higgs couplings $c_{tA,tW,t\varphi}^I$, as well as the semi-leptonic operators $c_{t,b}^{S(e)}$ and $c_t^{T(e)}$. Of the semi-leptonic operators the tensor operator induces the electron EDM through a single top loop, while the scalar ones require additional loops. The relevant RGEs are given by [87, 88],

$$\frac{d}{d \ln \mu} \begin{pmatrix} d_e \\ c_t^{SI(e)}/\Lambda^2 \\ c_t^{TI(e)}/\Lambda^2 \\ c_b^{SI(e)}/\Lambda^2 \end{pmatrix} = \frac{1}{(4\pi)^2} \begin{pmatrix} 0 & 0 & -16N_C Q_t m_t & 0 \\ 0 & -6C_F g_S^2 & 0 & 2(1 - N_c) y_t y_b \\ 0 & \frac{3}{8} g_W^2 + \frac{5}{8} g_Y^2 & 2C_F g_S^2 & 0 \\ 0 & 0 & 0 & -6C_F g_S^2 \end{pmatrix} \cdot \begin{pmatrix} d_e \\ c_t^{SI(e)}/\Lambda^2 \\ c_t^{TI(e)}/\Lambda^2 \\ c_b^{SI(e)}/\Lambda^2 \end{pmatrix}, \quad (65)$$

where $C_F = (N_C^2 - 1)/2N_C$, $y_{b,t} = m_{b,t}\sqrt{2}/v$, Q_f stands for the electric charge, and we only kept the electroweak terms that are relevant for the mixing of $c_{t,b}^{SI(e)}$ into $c_t^{TI(e)}$. The solution of the above equations provides the leading logarithmic contributions to the electron EDM. These, combined with $d_e \leq 8.7 \cdot 10^{-16} \text{ e fm}$ [95], give stringent constraints, which are again collected in Table 5. The same loops that induce the electron EDM also give a contribution to the electron anomalous magnetic moment, proportional to the real part of the semileptonic couplings. Although the resulting limits are weaker than the EDM limits they are still significant for two of the couplings, we obtain $|c_t^{S(e)}| \lesssim 2 \cdot 10^{-2}$ and $|c_t^{T(e)}| \lesssim 3 \cdot 10^{-5}$.

Of the top-Higgs couplings, $c_{t\varphi}^I$ generates the electron EDM through two-loop Barr-Zee diagrams [82–85], giving a stronger limit than the neutron EDM. In addition, when we evolve the $c_{tA,tW}^I$ couplings from the scale of new physics, Λ , to lower energies they first mix into CPV Higgs-gauge couplings of the form $(\varphi^\dagger \varphi) \tilde{X}_{\mu\nu} X^{\mu\nu}$ [88, 96, 97], where X denotes an $SU(2)$ or $U(1)$ gauge-field strength. In a second step these gauge-Higgs couplings mix into the electron and light-quark EDMs. This last step is proportional to the Yukawa couplings of the light fields leading to a strong suppression. Nevertheless, the experimental limit on the electron EDM is sufficiently strong to overwhelm the other probes of the CPV components of these two top-quark dipoles [88, 96].

Finally, we briefly discuss limits from rare B decays. At the one-loop level, the couplings $c_{\varphi tb,bW,tA,tW}^I$ give contributions to flavour-changing dipole operators that mediate $b \rightarrow s$ transitions proportional to the CKM element $V_{ts} \simeq 0.04$. The contributions of these flavour-changing operators to the CP asymmetry $A_{CP}(B \rightarrow X_s \gamma)$ [98], together with the experimental measurement [99], can be used set the limits in Table 5. It should be noted that measurements of the branching ratio can constrain the real parts of these couplings as well. This leads to limits which are typically a factor of a few stronger than those on the imaginary parts, see, for example, Refs. [80, 100–102].

Four-heavy

$c_{QtQb}^I \equiv \text{Im}\{C_{quqd}^{1(3333)}\}$	$[-3.4, 3.4] \cdot 10^{-3}$	(d_n)
$c_{QtQb}^{8I} \equiv \text{Im}\{C_{quqd}^{8(3333)}\}$	$[-2.2, 2.2] \cdot 10^{-2}$	(d_n)

Two-heavy

$c_{t\varphi}^I \equiv \text{Im}\{C_{u\varphi}^{(33)}\}$	$[-3.7, 3.7]$	(d_n)	$[-0.18, 0.18]$	(d_e)
$c_{\varphi tb}^I \equiv \text{Im}\{C_{\varphi ud}^{(33)}\}$	$[-0.019, 0.019]$	(d_n)	$[-0.052, 0.052]$	$(B \rightarrow X_s \gamma)$
$c_{tW}^I \equiv \text{Im}\{C_{uW}^{(33)}\}$	$[-8.1, 8.1] \cdot 10^{-3}$	(d_e)	$[-2.4, 4.5]$	$(B \rightarrow X_s \gamma)$
$c_{tA}^I \equiv \text{Im}\{c_W C_{uB}^{(33)} + s_W C_{uW}^{(33)}\}$	$[-6.3, 6.3] \cdot 10^{-3}$	(d_e)	$[-9.0, 5.0]$	$(B \rightarrow X_s \gamma)$
$c_{bW}^I \equiv \text{Im}\{C_{dW}^{(33)}\}$	$[-5.5, 5.5] \cdot 10^{-4}$	(d_n)	$[-4.3, 2.3] \cdot 10^{-2}$	$(B \rightarrow X_s \gamma)$
$c_{tG}^I \equiv \text{Im}\{C_{uG}^{(33)}\}$	$[-6.9, 6.9] \cdot 10^{-3}$	(d_n)		

Two-heavy-two-lepton

$c_t^{SI(e)} \equiv \text{Im}\{C_{lequ}^{1(1133)}\}$	$[-5.5, 5.5] \cdot 10^{-8}$	(d_e)
$c_t^{TI(e)} \equiv \text{Im}\{C_{lequ}^{3(1133)}\}$	$[-8.0, 8.0] \cdot 10^{-11}$	(d_e)
$c_b^{SI(e)} \equiv \text{Im}\{C_{ledq}^{(1133)}\}$	$[-2.5, 2.5] \cdot 10^{-4}$	(d_e)

Table 5: Constraints from the electron and neutron EDMs as well as $A_{CP}(B \rightarrow X_s \gamma)$. Here we turn on one coupling at a time and assume $\Lambda = 1$ TeV. The source of the constraints are indicated in brackets.

Summary

All the above discussed constraints are collected in Table 5. With the exception of $c_{t\varphi}^I$, the CPV coefficients are constrained at the percent level or stronger by EDM experiments. The semi-leptonic operators are more stringently constrained, which is mainly due to the fact that their contribution to d_e is proportional to m_t (where one would naively expect m_e). Instead, the constraints from $B \rightarrow X_s \gamma$ are particularly strong for the c_{bW}^I and $c_{\varphi tb}^I$ couplings because of an m_t/m_b enhancement. In most cases, the constraints on the imaginary parts are stronger than the corresponding limits on the real parts of the top-quark couplings. As a result, it will be difficult to reach a similar sensitivity by studying CPV observables at the LHC.

The interpretation of these low-energy constraints requires some care however. In deriving these limits we have assumed one dimension-six operator to be present at the scale Λ at a time. This assumption is no longer valid if multiple top operators are important at the scale Λ , or if one makes less restrictive assumptions about the flavor structure, such as a non-linear flavor symmetry [18]. A global analysis involving all top-quark operators, for example, would leave some combinations of operator coefficients unconstrained [88]. The difference between *individual* and *global* constraints is typically large for the CPV components as only a handful of sensitive low-energy measurements exist, in contrast to a much larger range of high-energy measurements of the real components. In a global setting, collider constraints on the CPV Wilson coefficients are therefore necessary to bound unconstrained directions in the parameter space. An example is the recent ATLAS measurement [103] of a CPV phase in $t \rightarrow bW$ decays which significantly impacts the global fit of CPV top-Higgs interactions [88, 89].

In addition, the low-energy observables get contributions from SMEFT operators that do not involve top quarks. For example, if an electron EDM is generated at the scale Λ with exactly the right size, it could weaken the limits on the semi-leptonic operators significantly. In fact, the leading logarithmic contributions we considered here result from divergent loops and require non-top operators, such as d_e , to absorb the divergences. In these cases one might expect $d_e(\Lambda) \neq 0$, which could in principle lead to cancellations and weakened limits. These cancellations have to be very severe in order to avoid the strong low-energy constraints. In any case, in order to evade the low-energy limits strong correlations between SMEFT operators are required, and this would

pose highly non-trivial constraints on models of beyond-the-SM physics.

B UFO models

The `dim6top` implementation of the degrees of freedom introduced in this note, as well as the `SMEFTsim` implementation of Warsaw-basis operators will be described in this appendix. Such UFO [104] models can be used for Monte Carlo simulation.

B.1 The `dim6top` implementation

The flavour-, B - and L -conserving parameters implemented in the `dim6top` UFO model (available at <https://feynrules.irmp.ucl.ac.be/wiki/dim6top>) are listed in Table 6. The FCNC degrees of freedom defined in Appendix E and implemented in this model are listed in Table 7.

General comments

- The implementation is a tree-level one.
- Λ is conventionally fixed to 1 TeV. Equivalently, EFT input parameters can be thought of as being the dimensionful $\tilde{c}_i \equiv c_i/\Lambda^2$ expressed in units of TeV^{-2} .
- The CKM matrix is assumed to be a unit matrix.
- The masses of u, d, s, c, e, μ fermions are set to zero by default.
- The unitary gauge is used and Goldstone bosons are removed.
- Are only added to the Lagrangian, the Hermitian conjugates of the non-Hermitian operators, and independent flavour assignments.
- Two versions of the model are made available. In the first one, `dim6top_LO_UFO`, all the flavour-, B - and L -conserving parameters are assigned the same *coupling order*: `DIM6=1`. Similarly, all the flavour-changing parameters are assigned one single *coupling order*: `FCNC=1`.

In a second version, `dim6top_LO_UFO_each_coupling_order`, an individual *coupling order* is additionally assigned to each EFT parameter: the `cQQ1` and `cqq11x3331` parameters are for instance assigned `DIM6_cQQ1` and `FCNC_cqq11x3331` *coupling orders*.

This allows for the selection of individual degrees-of-freedom interferences in `MG5_aMC@NLO`, using a syntax such as

```
> generate p p > t t~ FCNC=0 DIM6^2==1 DIM6_ctZ^2==1
> generate p p > t t~ FCNC=0 DIM6^2==2 DIM6_ctZ^2==1 DIM6_ctW^2==1
```

which would for instance respectively yield the interference between SM amplitudes and that in which `ctZ` is inserted once, and between amplitudes in which `ctZ` and `ctW` are inserted once. Specifying the order of the squared amplitude is however not supported yet when decay chains are specified.

A positive `QED=n` *coupling order* has also been assigned to EFT parameters corresponding to operators involving n Higgs doublet fields in the unbroken phase. Given that the Higgs vacuum expectation value has `QED=-1`, this avoids technical problems related to the appearance of interactions with net negative `QED` *coupling order*.

Syntax

- In `MG5_aMC@NLO`, import the model by


```
> import model dim6top_LO_UFO, or
> import model dim6top_LO_UFO_each_coupling_order
```
- By default, the bottom quark is massive and the four-flavour scheme is used. Loading the model with a restriction card where `MB=0` would automatically switch to the five flavour scheme. One can otherwise redefine manually:

Four-heavy	
c_{QQ}^1	cQQ1
c_{QQ}^8	cQQ8
c_{Qt}^1	cQt1
c_{Qt}^8	cQt8
c_{Qb}^1	cQb1
c_{Qb}^8	cQb8
c_{tt}^1	ctt1
c_{tb}^1	ctb1
c_{tb}^8	ctb8
$c_{QtQb}^{1[I]}$	cQtQb1 [I] (I stands for imaginary part)
$c_{QtQb}^{8[I]}$	cQtQb8 [I]
Two-heavy-two-light	
$c_{Qq}^{3,1}$	cQq13 $U(2)_q \times U(2)_u \times U(2)_d$ assumed
$c_{Qq}^{3,8}$	cQq83
$c_{Qq}^{1,1}$	cQq11
$c_{Qq}^{1,8}$	cQq81
c_{Qu}^1	cQu1
c_{Qu}^8	cQu8
c_{Qd}^1	cQd1
c_{Qd}^8	cQd8
c_{tq}^1	ctq1
c_{tq}^8	ctq8
c_{tu}^1	ctu1
c_{tu}^8	ctu8
c_{td}^1	ctd1
c_{td}^8	ctd8
Two-heavy	
$c_{t\varphi}^{[I]}$	ctp, ctpI
$c_{\varphi Q}^3$	cpQM
$c_{\varphi Q}^8$	cpQ3
$c_{\varphi t}$	cpt
$c_{\varphi b}$	cpb (implemented but involves no top)
$c_{\varphi tb}^{[I]}$	cptb, cptbI
$c_{\varphi W}^{[I]}$	ctW, ctWI
$c_{\varphi Z}^{[I]}$	ctZ, ctZI
$c_{bW}^{[I]}$	cbW, cbWI
$c_{tG}^{[I]}$	ctG, ctGI
Two-heavy-two-lepton	
$c_{Ql}^{3(\ell)}$	cQl3(1) assuming lepton flavour diagonality:
$c_{Ql}^{(\ell)}$	cQlM(1) ($1 \in \{1, 2, 3\}$)
$c_{Qe}^{(\ell)}$	cQe
$c_{tl}^{(\ell)}$	ctl(1)
$c_{te}^{(\ell)}$	cte(1)
$c_t^{S[I](\ell)}$	ct1S [I] (1)
$c_t^{T[I](\ell)}$	ct1T [I] (1)
$c_b^{S[I](\ell)}$	cb1S [I] (1)
Two-heavy-two-light, preserving only $U(2)_{q+u+d}$	
$c_{tQqu}^{1[I]}$	ctQqu1 [I]
$c_{tQqu}^{8[I]}$	ctQqu8 [I]
$c_{bQqd}^{1[I]}$	cbQqd1 [I]
$c_{bQqd}^{8[I]}$	cbQqd8 [I]
$c_{Qtqd}^{1[I]}$	cQtqd1 [I]
$c_{Qtqd}^{8[I]}$	cQtqd8 [I]
$c_{Qbqu}^{1[I]}$	cQbqu1 [I]
$c_{Qbqu}^{8[I]}$	cQbqu8 [I]
$c_{btud}^{1[I]}$	cbtud1 [I]
$c_{btud}^{8[I]}$	cbtud8 [I]

Table 6: dim6_{top} UFO model parameter names for the flavour-, B - and L -conserving degrees of freedom defined in [Appendices C](#) and [D](#).

One-light-three-heavy		
$c_{qq}^{1[I](333a)}$	cqq11 [I] x333 (a)	(a) $\in \{1, 2\}$: light quark gen.
$c_{qq}^{3[I](333a)}$	cqq13 [I] x333 (a)	I: imaginary part
$c_{uu}^{[I](333a)}$	cuu1 [I] x333 (a)	
$c_{qu}^{1[I](333a)}$	cqu1 [I] x333 (a)	
$c_{qu}^{8[I](333a)}$	cqu8 [I] x333 (a)	
$c_{qu}^{1[I](3a33)}$	cqu1 [I] x3 (a) 33	
$c_{qu}^{8[I](3a33)}$	cqu8 [I] x3 (a) 33	
$c_{qd}^{1[I](333a)}$	cqd1 [I] x333 (a)	
$c_{qd}^{8[I](333a)}$	cqu8 [I] x333 (a)	
$c_{qd}^{1[I](3a33)}$	cqd1 [I] x3 (a) 33	
$c_{qd}^{8[I](3a33)}$	cqd8 [I] x3 (a) 33	
$c_{ud}^{1[I](333a)}$	cud1 [I] x333 (a)	
$c_{ud}^{8[I](333a)}$	cud8 [I] x333 (a)	
$c_{ud}^{1[I](3a33)}$	cud1 [I] x3 (a) 33	
$c_{ud}^{8[I](3a33)}$	cud8 [I] x3 (a) 33	
$c_{quqd}^{1[I](333a)}$	cquqd1 [I] x333 (a)	
$c_{quqd}^{1[I](33a3)}$	cquqd1 [I] x33 (a) 3	
$c_{quqd}^{1[I](3a33)}$	cquqd1 [I] x3 (a) 33	
$c_{quqd}^{1[I](a333)}$	cquqd1 [I] x (a) 333	
$c_{quqd}^{8[I](333a)}$	cquqd8 [I] x333 (a)	
$c_{quqd}^{8[I](33a3)}$	cquqd8 [I] x33 (a) 3	
$c_{quqd}^{8[I](3a33)}$	cquqd8 [I] x3 (a) 33	
$c_{quqd}^{8[I](a333)}$	cquqd8 [I] x (a) 333	
Three-light-one-heavy		
$c_{qq}^{1,1[I](3a)}$	cqq11 [I] x3 (a) ii	
$c_{qq}^{3,1[I](3a)}$	cqq13 [I] x3 (a) ii	
$c_{qq}^{1,8[I](3a)}$	cqq81 [I] x3 (a) ii	
$c_{qq}^{3,8[I](3a)}$	cqq83 [I] x3 (a) ii	
$c_{uu}^{1[I](3a)}$	cuu1 [I] x3 (a) ii	
$c_{uu}^{8[I](3a)}$	cuu8 [I] x3 (a) ii	
$c_{ud}^{1[I](3a)}$	cud1 [I] x3 (a) ii	
$c_{ud}^{8[I](3a)}$	cud8 [I] x3 (a) ii	
$c_{qu}^{1[I](3a)}$	cqu1 [I] x3 (a) ii	
$c_{qu}^{8[I](3a)}$	cqu8 [I] x3 (a) ii	
$c_{qu}^{1[I](a3)}$	cqu1 [I] xii3 (a)	
$c_{qu}^{8[I](a3)}$	cqu8 [I] xii3 (a)	
$c_{qd}^{1[I](3a)}$	cqd1 [I] x3 (a) ii	
$c_{qd}^{8[I](3a)}$	cqd8 [I] x3 (a) ii	
One-light-one-heavy		
$c_{t\varphi}^{[I](3a)}$	ctp [I] x3 (a)	
$c_{t\varphi}^{[I](a3)}$	ctp [I] x (a) 3	
$c_{\varphi q}^{-[I](3+a)}$	cpQM [I] x3 (a)	
$c_{\varphi q}^{3[I](3+a)}$	cpQ3 [I] x3 (a)	
$c_{\varphi q}^{[I](3+a)}$	cpt [I] x3 (a)	
$c_{\varphi u}^{[I](3a)}$	cptb [I] x3 (a)	
$c_{\varphi ud}^{[I](a3)}$	cptb [I] x (a) 3	
$c_{\varphi uW}^{[I](a3)}$	ctW [I] x3 (a)	
$c_{\varphi uW}^{[I](3a)}$	ctW [I] x (a) 3	
$c_{\varphi uZ}^{[I](3a)}$	ctZ [I] x3 (a)	
$c_{\varphi uZ}^{[I](a3)}$	ctZ [I] x (a) 3	
$c_{\varphi dW}^{[I](3a)}$	cdW [I] x3 (a)	
$c_{\varphi dW}^{[I](a3)}$	cdW [I] x (a) 3	
$c_{\varphi dG}^{[I](3a)}$	cdG [I] x3 (a)	
$c_{\varphi dG}^{[I](a3)}$	cdG [I] x (a) 3	
One-light-one-heavy-two-lepton		
$c_{lq}^{3(\ell,3+a)}$	cQl3 [I] x(1) x3 (a)	(1) $\in \{1, 2, 3\}$ lepton gen.
$c_{lq}^{(\ell,3+a)}$	cQlM [I] x(1) x3 (a)	
$c_{eq}^{(\ell,3+a)}$	cQe [I] x(1) x3 (a)	
$c_{tu}^{(\ell,3+a)}$	ctl [I] x(1) x3 (a)	
$c_{eu}^{(\ell,3+a)}$	cte [I] x(1) x3 (a)	
$c_{lequ}^{S(\ell,3a)}$	ct1S [I] x(1) x3 (a)	
$c_{lequ}^{S(\ell,a3)}$	ct1S [I] x(1) x (a) 3	
$c_{lequ}^{T(\ell,3a)}$	ct1T [I] x(1) x3 (a)	
$c_{lequ}^{T(\ell,a3)}$	ct1T [I] x(1) x (a) 3	
$c_{lequ}^{S(\ell,3a)}$	cb1S [I] x(1) x3 (a)	(implemented but involve
$c_{lequ}^{S(\ell,a3)}$	cb1S [I] x(1) x (a) 3	no top FCNC)

Table 7: dim6_{top} UFO model parameter names for the FCNC degrees of freedom introduced in [Appendix E](#).


```
> define p = p b b~
> define j = p
```

and set MB=0 in the `param_card`. For consistency, one may then also set `ymb=0`.

- Processes can be generated through commands like

```
> generate p p > t t~ FCNC=0 DIM6=1
```

which allows for one (or no) insertion of a parameter of DIM6 *coupling order* per amplitude.
- To focus on the leading QCD amplitudes, one can also restrict their maximal allowed QED order using for instance:

```
> generate p p > t t~ FCNC=0 DIM6=1 QED=0
> generate p p > t t~ Z FCNC=0 DIM6=1 QED=1
```

B.2 The SMEFTsim implementation

The SMEFTsim package [105] (available at <http://feynrules.irmp.ucl.ac.be/wiki/SMEFT>) provides a complete FeynRules [106] implementation of the B -conserving dimension-six Lagrangian in the Warsaw basis [1], that automatically performs the field and parameter redefinitions required to have canonically normalized kinetic terms and following from the choice of an input parameters set. The package contains FeynRules models as well as pre-exported UFO models for six different Lagrangians, corresponding to two possible input parameters sets ($\{\hat{\alpha}_{ew}, \hat{m}_Z, \hat{G}_F\}$ or $\{\hat{m}_W, \hat{m}_Z, \hat{G}_F\}$) and to three possible assumptions on the flavour structure of the theory:

- a **flavour general** case, in which all the flavour indices are explicitly kept and the Wilson coefficients of the fermionic operators are defined as tensorial parameters.
- a $U(3)^5$ **flavour symmetric** case in which flavour contractions are fixed by the symmetry. The Yukawa couplings are treated as flavour-breaking spurions and consistently inserted in operators with chirality-flipping fermion currents.
- a **linear MFV** case [17] that, unlike the $U(3)^5$ symmetric setup, does not contain CP violating parameters beyond the CKM phase while it includes insertions of the flavour-violating spurions $Y_f Y_f^\dagger, Y_f^\dagger Y_f$ up to linear order.

Two versions of SMEFTsim are available, denominated “set A” and “set B”: these implementations are independent but completely equivalent, and their simultaneous availability is meant to help a cross-check of the results.

General comments

- Analogously to `dim6top`, SMEFTsim is a leading order, unitary gauge implementation.
- The Wilson coefficients are dimensionless quantities and the EFT cutoff Λ is an external parameter of the UFO, set by default to 1 TeV (`LambdaSMEFT = 1.e+03`).
- The definitions of the relevant parameters (in the Warsaw basis) are given in Table 8. The correspondence with the parameters used in `dim6top` can be deduced from the definitions summarized in Table 1.
A `QED=-1` interaction order has been assigned to `LambdaSMEFT`, in order to avoid couplings with negative QED order.⁶
- Complex Wilson coefficients are parametrized by their absolute value and complex phase `ciAbs Exp[I ciPh]` rather than by real and imaginary parts. When testing the imaginary part of a given operator it is therefore necessary to set the corresponding phase to $\pi/2 = 1.570796$.

⁶One coupling with negative QED order is still present nonetheless, namely the C_φ correction to the h^3 vertex, which plays no role here.

$C_{u\varphi}^{(33)}$	cuHAbs33, cuHPh33	$C_{\varphi u}^{(33)}$	cHuAbs33, cHuPh33
$C_{\varphi q}^{1(33)}$	chq1Abs33	$C_{\varphi q}^{3(33)}$	chq3Abs33
$C_{\varphi ud}^{(33)}$	chudAbs33, chudPh33		
$C_{uW}^{(33)}$	cuWAbs33, cuWPh33	$C_{dW}^{(33)}$	cdWAbs33, cdWPh33
$C_{uB}^{(33)}$	cuBAbs33, cuBPh33	$C_{uG}^{(33)}$	cuGAbs33, cuGPh33
$C_{qq}^{1(3333)}$	cqq1Abs3333	$C_{qq}^{3(3333)}$	cqq3Abs3333
$C_{(aa33)}^{1(aa33)}$	cqq1Abs(aa)33	$C_{(aa33)}^{3(aa33)}$	cqq3Abs(aa)33
$C_{(a33a)}^{1(a33a)}$	cqq1Abs(a)33(a)	$C_{(a33a)}^{3(a33a)}$	cqq3Abs(a)33(a)
$C_{qq}^{1(3333)}$	cqu1Abs3333	$C_{qq}^{8(3333)}$	cqu8Abs3333
$C_{(aa33)}^{1(aa33)}$	cqu1Abs(aa)33	$C_{(aa33)}^{8(aa33)}$	cqu8Abs(aa)33
$C_{(33aa)}^{1(33aa)}$	cqu1Abs33(aa)	$C_{(33aa)}^{8(33aa)}$	cqu8Abs33(aa)
$C_{qd}^{1(3333)}$	cqd1Abs3333	$C_{qd}^{8(3333)}$	cqd8Abs3333
$C_{(33aa)}^{1(33aa)}$	cqd1Abs33(aa)	$C_{(33aa)}^{8(33aa)}$	cqd8Abs33(aa)
$C_{uu}^{(3333)}$	cuuAbs3333	$C_{uu}^{8(3333)}$	cuu8Abs3333
$C_{(a33a)}^{(a33a)}$	cuuAbs(a)33(a)		
$C_{ud}^{1(3333)}$	cud1Abs3333	$C_{ud}^{8(3333)}$	cud8Abs3333
$C_{(33aa)}^{1(33aa)}$	cud1Abs33(aa)	$C_{(33aa)}^{8(33aa)}$	cud8Abs33(aa)
$C_{quqd}^{1(3333)}$	cquqd1Abs3x3x3x3, cquqd1Ph3x3x3x3	$C_{quqd}^{8(3333)}$	cquqd8Abs3x3x3x3, cquqd8Ph3x3x3x3
$C_{lq}^{1(l133)}$	clq1Abs(11)33	$C_{lq}^{3(l133)}$	clq3Abs(11)33
$C_{lu}^{(l133)}$	cluAbs(11)33	$C_{eq}^{(l133)}$	cqeAbs33(11)
$C_{eu}^{(l133)}$	ceuAbs(11)33	$C_{lequ}^{1(l133)}$	clequ1Abs(1)x(1)x3x3, clequ1Ph(1)x(1)x3x3
$C_{lequ}^{3(l133)}$	clequ3Abs(1)x(1)x3x3, clequ3Ph(1)x(1)x3x3	$C_{ledq}^{(l133)}$	cledqAbs(1)x(1)x3x3, cledqPh(1)x(1)x3x3

Table 8: Flavour conserving parameters in the SMEFTsim-A UFO implementation, that are in direct correspondence with the degrees of freedom defined in Appendix C. The index $a = \{1, 2\}$ runs over the light quark generations, while $l = \{1, 2, 3\}$ indicates lepton flavours.

flavour case	relevant parameters	total number
general	$[C_{uH}, C_{uB}, C_{uW}, C_{uG}]_{i3,3j}$, $[C_{dW}, C_{Hud}]_{3j}$, $[C_{Hu}, C_{Hq}^{(1),(3)}]_{i3}$, $[C_{qq}^{(1),(3)}, C_{uu}, C_{qu}^{(1),(8)}]_{3jkl,i3kl,ij3l,ijk3}$, $[C_{ud}^{(1),(8)}, C_{qe}, C_{qd}^{(1),(8)}]_{3jkl,i3kl}$, $[C_{lq}^{(1),(3)}, C_{eu}, C_{lu}, C_{lequ}^{(1),(3)}]_{ij3l,ijk3}$, $[C_{ledq}]_{ijk3}$, $[C_{quqd}^{(1),(8)}]_{3jkl,i3kl,ij3l}$ $C_{H\Box}, C_{HD}, C_{HWB}, [C_{U}]_{1221}, [C_{Hl}^{(3)}]_{11,22}$	618 abs. values 557 phases
$U(3)^5$	$C_{uH}, C_{Hu}, C_{Hq}^{(1),(3)}, C_{Hud}, C_{uW}, C_{uB}, C_{uG}, C_{dW}, C_{qq}^{(1),(3)}, C_{qq}^{(1),(3)'} ,$ $C_{lq}^{(1),(3)}, C_{uu}, C_{uu}, C_{ud}^{(1),(8)}, C_{eu}, C_{lu}, C_{qe}, C_{qu}^{(1),(8)}, C_{qd}^{(1),(8)}, C_{quqd}^{(1),(8)},$ $C_{H\Box}, C_{HD}, C_{HWB}, C_{U}, C_{U}', C_{Hl}^{(3)}$	34 abs. values 8 phases
linear MFV	$C_{uH}, C_{Hu}^*, C_{Hq}^{(1),(3)**}, C_{Hud}, C_{uW}, C_{uB}, C_{uG}, C_{dW}, C_{qq}^{(1),(3)****},$ $C_{qq}^{(1),(3)l****}, C_{lq}^{(1),(3)**}, C_{uu}^*, C_{uu}^l, C_{ud}^{(1),(8)**}, C_{eu}^*, C_{lu}^*, C_{qe}^*,$ $C_{qu}^{(1),(8)***}, C_{qd}^{(1),(8)***}, C_{quqd}^{(1),(8)}$, $C_{H\Box}, C_{HD}, C_{HWB}, C_{U}, C_{U}', C_{Hl}^{(3)}$	83 abs. values

Table 9: Detailed list of the parameters that are relevant for top-quark physics for each flavour assumption in SMEFTsim. These are all set to 1 when importing the `restrict_TopEFT` restriction in any given model. The indices i, j, k, l take values in $\{1, 2, 3\}$. The terms in the last rows are included as they contribute to top couplings via parameter redefinitions. In the MFV case all the parameters are real and coefficients with n asterisks admit n independent insertions of flavour-violating spurions.

- The SM couplings of the Higgs boson that first arise at loop level (i.e. hgg , $h\gamma\gamma$, $hZ\gamma$) are included and parametrized as effective vertices with a coefficient that reproduces the SM loop function. These vertices are assigned an interaction order `SMHLOOP = 1`.
- All the flavour contractions are automatically implemented in the model, with a parametrization that allows to fix only the independent ones. This means that, for instance, setting $C_{qq}^{1(aa33)} = 1$ introduces both the $O_{qq}^{1(aa33)}$ and $O_{qq}^{1(33aa)}$ terms in the Lagrangian.
- An interaction order `NP=1` has been defined for the Wilson coefficients, equivalent to `DIM6` in `dim6top`. There is no analogue of FCNC nor of the individual `DIM6_ci`.

Syntax

- In `MG5_aMC@NLO` import the model, restricted by the file `restrict_XXX.dat` by


```
> import model SMEFTsim_A_general_alphaScheme-XXX
```

 All the restrictions available leave `MB` and `ymb` non-vanishing. It is possible to switch to the five flavour scheme either modifying manually the restriction card or setting


```
> define p = p b b~
> define j = p
```

 after importing the model and then modifying the `param_card` after generating the process output.
- Processes can be generated with


```
> generate p p > t t~ NP==1 SMHLOOP=0
```

 to allow the insertion of one Wilson coefficient in the amplitude and excluding SM hgg , $h\gamma\gamma$, and $hZ\gamma$ vertices or, for instance, with


```
> generate p p > t t~ NP^2==1 SMHLOOP=0
```

 to select for the interference term. QED and QCD interaction orders can also be specified to select for specific diagrams. To ensure the inclusion of all the tree-level SM contributions, it is advisable to specify `QED<=8 QCD<=8`.

B.3 Benchmark results

The linear and quadratic EFT dependences of some total rates are displayed in [Tables 10-21](#). These are meant to provide benchmark results against which simulation procedures could be checked. They are also indicative of which degree of freedom is relevant for which process.

These numbers are obtained using `MG5_aMC@NLO` (v2.6.0 or 2.6.1) [40] for the 13 TeV LHC, with `nn23l01` as PDF set. All fermion masses and Yukawa couplings but the top ones (`MT=172`) are taken vanishing. The five-flavour scheme, default running renormalization and factorization scales are used, and simple $p_T > 20$ GeV, $|\eta| < 2.5$, $\Delta R > 0.4$ generation cuts are imposed on (b -)jets, charged leptons and photons.

All tree-level contributions are included irrespectively of their QED order. Additional dependences may also be generated: with finite fermion masses and Yukawas (especially the bottom ones), when considering other observables (e.g., sensitive to CPV contributions), beyond the tree level (e.g., at NLO in QCD or when accounting for loop-induced Higgs couplings), etc. Cuts may also affect the hierarchies of sensitivities.

Obtained with `dim6top`, these benchmark results have been cross checked with `SMEFTsim_A` version 2.0, in the flavour general setup and with the $\{\hat{\alpha}_{ew}, \hat{m}_Z, \hat{G}_F\}$ input scheme (equally valid results can be obtained with set B and/or switching to a $\{\hat{m}_W, \hat{m}_Z, \hat{G}_F\}$ input scheme):

- A set of dedicated restriction cards is provided with the `SMEFTsim_A_general_alphaScheme` model to reproduce these numerical results. All of them set to zero the masses and Yukawa couplings of all fermions except the bottom and top quarks. They also approximate the CKM matrix by a unit matrix and fix the input parameters to values consistent with those adopted in `dim6top`. In particular they modify

$$\begin{aligned} \text{MB} &= \text{ymb} = 4.7, & \text{MT} &= 172.0, & \text{MH} &= 125.0, & \text{MW} &= 79.824360 \\ \text{aEW} &= 7.818608\text{e-}03, & \text{aS} &= 0.1184 \end{aligned}$$

compared to the default settings. In addition:

restrict_Smlimit_top: sets to zero all the Wilson coefficients. This restriction is available for all the flavour setups.

restrict_TopEFT: sets to 1 the absolute values of all the Wilson coefficients that are relevant for top physics and to 0 the remaining ones. This restriction is available for all the flavour setups, and the list of coefficients retained in each case is given in [Table 9](#).

restrict_(ci)_top: with (ci) one of the degrees of freedom of [Table 6](#) in the notation of **dim6top**: turns on the combination of Wilson coefficients equivalent to setting $\text{ci} = 1$, while vanishing the others.

- As **dim6top** does not include loop-level interactions of the Higgs (hgg , $h\gamma\gamma$, or $hZ\gamma$), a meaningful comparison with **SMEFTsim** would require setting $\text{SMHLOOP}=0$.
- **SMEFTsim** utilizes the opposite convention, compared to **dim6top**, for the sign of covariant derivatives (schematically: $D_\mu = \partial_\mu + iA_\mu$). At the linear level, some interferences with SM amplitudes are affected, in particular those proportional to $\text{ctW}[\text{I}]$ and $\text{ctZ}[\text{I}]$.
- Due to different choices concerning the inclusion of non-independent flavour contractions (only independent flavour assignments are included in **dim6top** while all are in **SMEFTsim**), factor-of-two differences arise when considering the coefficients cQq83 , cQq81 , cQq13 , cQq11 , ctu1 , ctu8 , that stem from operators with four identical fields: $Q_{qq}^{1,3}$, O_{uu} .
- Due to the different parametrization of complex coefficients (in (Abs, Arg) rather than (Re, Im)), the evaluation of S_i^k for purely imaginary coefficients can be less accurate in **SMEFTsim**.
- In **SMEFTsim**, due to the internal implementation of Warsaw basis operators instead of the degrees of freedom specific to top-quark physics, some small interferences may need to be obtained from cancellations between large contributions and thus suffer from larger numerical uncertainties. This concerns for instance the evaluation of the vanishing linear dependence on the colour octet cQq83 in single top production. Phenomenological consequences may be limited.

C Flavour-, B - and L -conserving degrees of freedom

Let us define the EFT degrees of freedom, operator category by operator category. We recommend to quote results in terms of these degrees of freedom. Their definitions, in terms of Warsaw-basis operator coefficients are also summarized in [Table 1](#).

C.1 Four-heavy operators

We consider first four-quark operators. All vector ($\bar{L}\bar{L}\bar{L}\bar{L}$, $\bar{L}\bar{L}\bar{R}\bar{R}$, $\bar{R}\bar{R}\bar{R}\bar{R}$) operators have real $C^{(3333)} = C^{(3333)*}$ coefficients, unlike the scalar ($\bar{L}\bar{R}\bar{L}\bar{R}$) ones. For $\bar{L}\bar{L}\bar{L}\bar{L}$ operators, one can define the colour singlet and octets that would or not interfere with the QCD amplitudes:⁷

$$\begin{pmatrix} O_{qq}^{1(3333)} \\ O_{qq}^{3(3333)} \end{pmatrix} = \begin{pmatrix} 1 & -1/3 \\ 0 & 4 \end{pmatrix}^T \begin{pmatrix} (\bar{Q}\gamma_\mu Q) (\bar{Q}\gamma^\mu Q) \\ (\bar{Q}\gamma_\mu T^A Q) (\bar{Q}\gamma^\mu T^A Q) \end{pmatrix}, \quad (66)$$

where Q represents the third-generation left-handed quark doublet, while t and b will represent the right-handed quark singlets in the unbroken electroweak phase. In the electroweak broken

⁷Note that we wrote matrix equations involving operators as $O = M^T o$. The Lagrangian $C^T O$ terms are then equated to $c^T o$ to establish the definition of the coefficients of the o operators as $c \equiv M C$.

phase, one further obtains:

$$\begin{pmatrix} O_{qq}^{1(3333)} \\ O_{qq}^{3(3333)} \end{pmatrix} = \begin{pmatrix} 1 & 1 \\ 2 & -2/3 \\ 0 & 8 \\ 1 & 1 \end{pmatrix}^T \begin{pmatrix} (\bar{t}\gamma^\mu P_L t)(\bar{t}\gamma_\mu P_L t) \\ (\bar{t}\gamma^\mu P_L t)(\bar{b}\gamma_\mu P_L b) \\ (\bar{t}\gamma^\mu T^A P_L t)(\bar{b}\gamma_\mu T^A P_L b) \\ (\bar{b}\gamma^\mu P_L b)(\bar{b}\gamma_\mu P_L b) \end{pmatrix} \quad (67)$$

which is useful to identify the colour singlet and octet combinations of two top and two b quarks, four tops and four b 's. We use the combinations leading to $\bar{t}t\bar{b}b$ interactions as independent degrees of freedom. No further manipulation is performed on other operators featuring four heavy quarks. One thus defines:

$$\begin{aligned} c_{Q_t}^1 &\equiv C_{qu}^{1(3333)}, & c_{Q_t}^8 &\equiv C_{qu}^{8(3333)}, & c_{tt}^1 &\equiv C_{uu}^{1(3333)}, & c_{tb}^1 &\equiv C_{ud}^{1(3333)}, \\ c_{Q_Q}^1 &\equiv 2C_{qq}^{1(3333)} - \frac{2}{3}C_{qq}^{3(3333)}, & c_{Q_t}^8 &\equiv C_{qu}^{8(3333)}, & c_{tt}^1 &\equiv C_{uu}^{1(3333)}, & c_{tb}^8 &\equiv C_{ud}^{8(3333)}, \\ c_{Q_Q}^8 &\equiv 8C_{qq}^{3(3333)}, & c_{Q_b}^1 &\equiv C_{qd}^{1(3333)}, & c_{tt}^8 &\equiv C_{uu}^{8(3333)}, & c_{tb}^8 &\equiv C_{ud}^{8(3333)}, \\ & & c_{Q_b}^8 &\equiv C_{qd}^{8(3333)}, & & & & \end{aligned} \quad (68)$$

and

$$c_{Q_t Q_b}^{1[I]} \equiv \frac{[\text{Im}]\{C_{quqd}^{1(3333)}\}}{\text{Re}}, \quad c_{Q_t Q_b}^{8[I]} \equiv \frac{[\text{Im}]\{C_{quqd}^{8(3333)}\}}{\text{Re}}. \quad (69)$$

In total, there are thus 11 + 2 CPV degrees of freedom for four-heavy operators. One can also define the combination $c_{Q_Q}^+ \equiv C_{qq}^{1(3333)} + C_{qq}^{8(3333)} = (3c_{Q_Q}^1 + c_{Q_Q}^8)/6$ which appears in front of operators involving four left-handed top and bottom quarks but is not independent of the ones defined above.

C.2 Two-light-two-heavy operators

Scalar operators involving a light-quark current are not allowed by our baseline flavour assumption (see Appendix D where this assumption is relaxed). The coefficients of the vector $\bar{L}\bar{L}\bar{L}\bar{L}$ operators $O_{qq}^{3,1}$ have the following symmetries under permutations of their generation indices:

$$C_{qq}^{(ijkl)} = C_{qq}^{(klij)}, \quad C_{qq}^{(jilk)} = C_{qq}^{(ijkl)*}, \quad (\text{and thus } C_{qq}^{(lkji)} = C_{qq}^{(ijkl)*}),$$

which namely implies that $C_{qq}^{(iijj)}$ and $C_{qq}^{(ijji)}$ elements are real. From the $C_{qq}^{(ijkl)}$ and $C_{qq}^{(klij)}$ combinations, only one is thus retained in the sum over flavour indices in the EFT Lagrangian of Eq. (34). For each of these two operators, there are thus two independent assignments of third-generation indices to a quark-antiquark pairs that are compatible with our $U(2)_q \times U(2)_u \times U(2)_d$ baseline flavour symmetry:

$$C_{qq}^{(ii33)} = C_{qq}^{(ii33)*} = C_{qq}^{(33ii)} = C_{qq}^{(33ii)*}, \quad C_{qq}^{(i33i)} = C_{qq}^{(i33i)*} = C_{qq}^{(3i3i)} = C_{qq}^{(3i3i)*}. \quad (70)$$

To understand better the structure of their interferences with SM amplitudes it is useful to decompose them, using Fierz identities, onto quadrilinears featuring a heavy- and a light-quark bilinear. One obtains:

$$\begin{pmatrix} O_{qq}^{1(3a ii)} \\ O_{qq}^{1(3i ia)} \\ O_{qq}^{3(3a ii)} \\ O_{qq}^{3(3i ia)} \end{pmatrix} = \begin{pmatrix} 1 & 1/6 & 0 & 1/2 \\ 0 & 1/6 & 1 & -1/6 \\ 0 & 1 & 0 & 3 \\ 0 & 1 & 0 & -1 \end{pmatrix}^T \begin{pmatrix} (\bar{Q}\gamma_\mu Q)(\bar{q}_i\gamma^\mu q_i) \\ (\bar{Q}\gamma_\mu \tau^I Q)(\bar{q}_i\gamma^\mu \tau^I q_i) \\ (\bar{Q}\gamma_\mu T^A Q)(\bar{q}_i\gamma^\mu T^A q_i) \\ (\bar{Q}\gamma_\mu T^A \tau^I Q)(\bar{q}_i\gamma^\mu T^A \tau^I q_i) \end{pmatrix}, \quad (71)$$

and similarly, for the $\bar{R}\bar{R}\bar{R}\bar{R}$ operator O_{uu} :

$$\begin{pmatrix} O_{uu}^{(ii33)} \\ O_{uu}^{(i33i)} \end{pmatrix} = \begin{pmatrix} 1 & 1/3 \\ 0 & 2 \end{pmatrix}^T \begin{pmatrix} (\bar{t}\gamma_\mu t)(\bar{u}_i\gamma^\mu u_i) \\ (\bar{t}\gamma_\mu T^A t)(\bar{u}_i\gamma^\mu T^A u_i) \end{pmatrix}. \quad (72)$$

There are four four-quark operators of $\bar{L}\bar{L}\bar{R}\bar{R}$ type in the Warsaw basis: $O_{qu}^{1(ijkl)}$, $O_{qu}^{8(ijkl)}$, $O_{qd}^{1(ijkl)}$, $O_{qd}^{8(ijkl)}$ which form six degrees of freedom when accounting for the two $C_{qu}^{(ii33)} = C_{qu}^{(ii33)*}$ and $C_{qu}^{(33ii)} = C_{qu}^{(33ii)*}$ flavour assignments. Altogether, one thus defines the following degrees of freedom for two-light-two-heavy operators:

$$\begin{aligned}
c_{Qq}^{1,1} &\equiv C_{qq}^{1(ii33)} + \frac{1}{6}C_{qq}^{1(i33i)} + \frac{1}{2}C_{qq}^{3(i33i)}, & c_{tu}^1 &\equiv C_{uu}^{(ii33)} + \frac{1}{3}C_{uu}^{(i33i)}, & c_{tq}^1 &\equiv C_{qu}^{1(ii33)}, \\
c_{Qq}^{3,1} &\equiv C_{qq}^{3(ii33)} + \frac{1}{6}(C_{qq}^{1(i33i)} - C_{qq}^{3(i33i)}), & c_{tu}^8 &\equiv 2C_{uu}^{(i33i)}, & c_{Qu}^1 &\equiv C_{qu}^{1(33ii)}, \\
c_{Qq}^{1,8} &\equiv C_{qq}^{1(i33i)} + 3C_{qq}^{3(i33i)}, & c_{td}^1 &\equiv C_{ud}^{1(33ii)}, & c_{Qd}^1 &\equiv C_{qd}^{1(33ii)}, \\
c_{Qq}^{3,8} &\equiv C_{qq}^{1(i33i)} - C_{qq}^{3(i33i)}, & c_{td}^8 &\equiv C_{ud}^{8(33ii)}, & c_{tq}^8 &\equiv C_{qu}^{8(ii33)}, \\
&&&&& c_{Qu}^8 &\equiv C_{qu}^{8(33ii)}, \\
&&&&& c_{Qd}^8 &\equiv C_{qd}^{8(33ii)},
\end{aligned} \tag{73}$$

where i is either 1 or 2. In total, there are thus 14 degrees of freedom for two-light-two-heavy operators.

C.3 Two-heavy operators

The operator involving two quarks and boson which possibly contain a top quark where listed in [Section 3](#). There are a few choices to be made in the definitions of the associated degrees of freedom, in view of the electroweak broken phase decomposition of $O_{\varphi q}$

$$\begin{pmatrix} O_{\varphi q}^{1(33)} \\ O_{\varphi q}^{3(33)} \end{pmatrix} = \begin{pmatrix} -1 & 1 \\ 1 & 1 \\ 0 & 1 \\ 0 & 1 \end{pmatrix}^T \begin{pmatrix} \frac{+e}{2s_W c_W} (\bar{t}\gamma^\mu P_L t) Z_\mu (v+h)^2 \\ \frac{-e}{2s_W c_W} (\bar{b}\gamma^\mu P_L b) Z_\mu (v+h)^2 \\ \frac{e}{s_W \sqrt{2}} (\bar{t}\gamma^\mu P_L b) W_\mu^+ (v+h)^2 \\ \frac{e}{s_W \sqrt{2}} (\bar{b}\gamma^\mu P_L t) W_\mu^- (v+h)^2 \end{pmatrix}, \tag{74}$$

and of electroweak dipole operators:

$$\begin{pmatrix} O_{uB}^{(33)} \\ O_{uW}^{(33)} \end{pmatrix} = \begin{pmatrix} c_W & s_W \\ -s_W & c_W \\ 0 & 2 \end{pmatrix}^T \begin{pmatrix} (\bar{t}\sigma^{\mu\nu} P_R t) A_{\mu\nu} (v+h) \\ (\bar{t}\sigma^{\mu\nu} P_R t) Z_{\mu\nu} (v+h) \\ (\bar{b}\sigma^{\mu\nu} P_R t) W_{\mu\nu}^- (v+h) \end{pmatrix}, \tag{75}$$

where s_W and c_W are the sine and cosine of the weak mixing angle (in the unitary gauge). Among the possible definitions, we choose to use as degrees of freedom the combinations that involve charged W , Z bosons and tops in the broken phase. In this sector, one thus defines:

$$\begin{aligned}
c_{\varphi Q}^- &\equiv C_{\varphi q}^{1(33)} - C_{\varphi q}^{3(33)}, & c_{tW}^{[I]} &\equiv \frac{[\text{Im}]}{\text{Re}} \{C_{uW}^{(33)}\}, \\
c_{\varphi Q}^3 &\equiv C_{\varphi q}^{3(33)}, & c_{tZ}^{[I]} &\equiv \frac{[\text{Im}]}{\text{Re}} \{-s_W C_{uB}^{(33)} + c_W C_{uW}^{(33)}\}, \\
c_{\varphi t}^{[I]} &\equiv \frac{[\text{Im}]}{\text{Re}} \{C_{u\varphi}^{(33)}\}, & c_{bW}^{[I]} &\equiv \frac{[\text{Im}]}{\text{Re}} \{C_{dW}^{(33)}\}, \\
c_{\varphi tb}^{[I]} &\equiv \frac{[\text{Im}]}{\text{Re}} \{C_{\varphi ud}^{(33)}\}, & c_{tG}^{[I]} &\equiv \frac{[\text{Im}]}{\text{Re}} \{C_{uG}^{(33)}\}.
\end{aligned} \tag{76}$$

On the other hand, the combination of $O_{\varphi q}^{1,3(33)}$ operators that modifies the SM coupling of the b quark to the Z is $c_{\varphi Q}^+ \equiv C_{\varphi q}^{3(33)} + C_{\varphi q}^{1(33)} = c_{\varphi Q}^- + 2c_{\varphi Q}^3$ and the combination appearing electromagnetic dipole of the top is $c_{tA}^{[I]} \equiv \frac{[\text{Im}]}{\text{Re}} \{c_W C_{uB}^{(33)} + s_W C_{uW}^{(33)}\} = (c_{tW}^{[I]} - c_W c_{tZ}^{[I]})/s_W$. In total, there are thus $9 + 6$ CPV degrees of freedom for two-heavy operators.

C.4 Two-heavy-two-lepton operators

Let us now address the definition of the degrees of freedom associated to the operators involving two quarks and two leptons. We decompose the $O_{lq}^{1,3}$ operators in the broken phase,

$$\begin{pmatrix} O_{lq}^{1(\ell\ell 33)} \\ O_{lq}^{3(\ell\ell 33)} \end{pmatrix} = \begin{pmatrix} 1 & 1 \\ 1 & -1 \\ 1 & -1 \\ 1 & 1 \\ 0 & 2 \\ 0 & 2 \end{pmatrix}^T \begin{pmatrix} (\bar{\nu}_\ell \gamma^\mu P_L \nu_\ell)(\bar{t} \gamma_\mu P_L t) \\ (\bar{\nu}_\ell \gamma^\mu P_L \nu_\ell)(\bar{b} \gamma_\mu P_L b) \\ (\bar{\ell} \gamma^\mu P_L \ell)(\bar{t} \gamma_\mu P_L t) \\ (\bar{\ell} \gamma^\mu P_L \ell)(\bar{b} \gamma_\mu P_L b) \\ (\bar{\nu}_\ell \gamma^\mu P_L \nu_\ell)(\bar{b} \gamma_\mu P_L t) \\ (\bar{\ell} \gamma^\mu P_L \nu_\ell)(\bar{t} \gamma_\mu P_L b) \end{pmatrix}, \quad (77)$$

and select as degrees of freedom the combinations that give rise to a top-quark interaction with a pair of charged leptons, and to charged currents. One therefore defines:

$$\begin{aligned} c_{Ql}^{-(\ell)} &\equiv C_{lq}^{1(\ell\ell 33)} - C_{lq}^{3(\ell\ell 33)}, & c_{tl}^{(\ell)} &\equiv C_{lu}^{(\ell\ell 33)}, & c_{te}^{(\ell)} &\equiv C_{eu}^{(\ell\ell 33)}, & c_t^{S[I](\ell)} &\equiv \frac{[\text{Im}]}{\text{Re}}\{C_{lequ}^{1(\ell\ell 33)}\}, \\ c_{Ql}^{3(\ell)} &\equiv C_{lq}^{3(\ell\ell 33)}, & c_{Qe}^{(\ell)} &\equiv C_{eq}^{(\ell\ell 33)}, & & & c_t^{T[I](\ell)} &\equiv \frac{[\text{Im}]}{\text{Re}}\{C_{lequ}^{3(\ell\ell 33)}\}, \\ & & & & & & c_b^{S[I](\ell)} &\equiv \frac{[\text{Im}]}{\text{Re}}\{C_{ledq}^{3(\ell\ell 33)}\}. \end{aligned} \quad (78)$$

These constitute $8 + 3$ CPV degrees of freedom, for each of the three generations of leptons.

D Less restrictive flavour symmetry

We examine here the consequences of relaxing the flavour symmetry among the first two generations of quarks from $U(2)_q \times U(2)_u \times U(2)_d$ to $U(2)_{q+u+d}$. New contributions are only generated in the two-light-two-heavy category of four-quark operators as flavour-diagonal chirality-flipping light quark-antiquark pairs as well as right-handed charged currents within the first generations are now allowed.

D.1 Four-quark $\bar{L}L\bar{R}R$ operators

For this category of operators, the $(i33i)$ and $(3i3i)$ flavour assignments become allowed:

$$C_{qu}^{1(i33i)} = C_{qu}^{1(3i3i)*}, \quad C_{qu}^{8(i33i)} = C_{qu}^{8(3i3i)*}, \quad (79)$$

$$C_{qd}^{1(i33i)} = C_{qd}^{1(3i3i)*}, \quad C_{qd}^{8(i33i)} = C_{qd}^{8(3i3i)*}. \quad (80)$$

Using Fierz identities, one then obtains:

$$\begin{pmatrix} O_{qu}^{1(i33i)} \\ O_{qu}^{8(i33i)} \end{pmatrix} = \begin{pmatrix} -2/3 & -8/9 \\ -4 & 2/3 \end{pmatrix}^T \begin{pmatrix} (\bar{t} \quad Q)(\bar{q}_i \quad u_i) \\ (\bar{t}\Gamma^A Q)(\bar{q}_i T^A u_i) \end{pmatrix} \quad (81)$$

and similarly for O_{qd} operators. The corresponding degrees of freedom

$$\begin{aligned} c_{tQqu}^{1[I]} &= \frac{[\text{Im}]}{\text{Re}} \left\{ -\frac{2}{3} C_{qu}^{1(i33i)} - \frac{8}{9} C_{qu}^{8(i33i)} \right\}, & c_{tQqu}^{8[I]} &= \frac{[\text{Im}]}{\text{Re}} \left\{ -4 C_{qu}^{1(i33i)} + \frac{2}{3} C_{qu}^{8(i33i)} \right\}, \\ c_{bQqd}^{1[I]} &= \frac{[\text{Im}]}{\text{Re}} \left\{ -\frac{2}{3} C_{qd}^{1(i33i)} - \frac{8}{9} C_{qd}^{8(i33i)} \right\}, & c_{bQqd}^{8[I]} &= \frac{[\text{Im}]}{\text{Re}} \left\{ -4 C_{qd}^{1(i33i)} + \frac{2}{3} C_{qd}^{8(i33i)} \right\}, \end{aligned} \quad (82)$$

are complex.

D.2 Four-quark $\bar{L}R\bar{L}R$ operators

The O_{quqd} operators belong to that category. Proceeding to the Fierz decomposition:

$$\begin{pmatrix} O_{quqd}^{1(i33i)} \\ O_{quqd}^{1(3ii3)} \\ O_{quqd}^{8(i33i)} \\ O_{quqd}^{8(3ii3)} \end{pmatrix} = \begin{pmatrix} -1/6 & 0 & -2/9 & 0 \\ -1 & 0 & 1/6 & 0 \\ -1/24 & 0 & -1/18 & 0 \\ -1/4 & 0 & 1/24 & 0 \\ 0 & -1/6 & 0 & -2/9 \\ 0 & -1 & 0 & 1/6 \\ 0 & -1/24 & 0 & -1/18 \\ 0 & -1/4 & 0 & 1/24 \end{pmatrix}^T \begin{pmatrix} (\bar{Q} & t) \varepsilon (\bar{q}_i & d_i) \\ (\bar{Q} & T^A t) \varepsilon (\bar{q}_i & T^A d_i) \\ (\bar{Q} \sigma_{\mu\nu} & t) \varepsilon (\bar{q}_i \sigma^{\mu\nu} & d_i) \\ (\bar{Q} \sigma_{\mu\nu} T^A & t) \varepsilon (\bar{q}_i \sigma^{\mu\nu} T^A & d_i) \\ (\bar{Q} & b) \varepsilon (\bar{q}_i & u_i) \\ (\bar{Q} & T^A b) \varepsilon (\bar{q}_i & T^A u_i) \\ (\bar{Q} \sigma_{\mu\nu} & b) \varepsilon (\bar{q}_i \sigma^{\mu\nu} & u_i) \\ (\bar{Q} \sigma_{\mu\nu} T^A & b) \varepsilon (\bar{q}_i \sigma^{\mu\nu} T^A & u_i) \end{pmatrix}, \quad (83)$$

one can for instance select the scalar operator coefficients as independent degrees of freedom:

$$\begin{aligned} c_{Qtqd}^{1[I]} &= \frac{[\text{Im}]}{\text{Re}} \left\{ -\frac{1}{6} C_{quqd}^{1(i33i)} - \frac{2}{9} C_{quqd}^{8(i33i)} \right\}, & c_{Qtqd}^{8[I]} &= \frac{[\text{Im}]}{\text{Re}} \left\{ -C_{quqd}^{1(i33i)} + \frac{1}{6} C_{quqd}^{8(i33i)} \right\}, \\ c_{Qbqu}^{1[I]} &= \frac{[\text{Im}]}{\text{Re}} \left\{ -\frac{1}{6} C_{quqd}^{1(3ii3)} - \frac{2}{9} C_{quqd}^{8(3ii3)} \right\}, & c_{Qbqu}^{8[I]} &= \frac{[\text{Im}]}{\text{Re}} \left\{ -C_{quqd}^{1(3ii3)} + \frac{1}{6} C_{quqd}^{8(3ii3)} \right\}, \end{aligned} \quad (84)$$

which are complex.

D.3 Four-quark $\bar{R}R\bar{R}R$ operators

In this category, new structures only arise for O_{ud} operators. The Fierz decomposition gives:

$$\begin{pmatrix} O_{ud}^{1(i33i)} \\ O_{ud}^{8(i33i)} \end{pmatrix} = \begin{pmatrix} 1/3 & 4/9 \\ 2 & -1/3 \end{pmatrix}^T \begin{pmatrix} (\bar{b}\gamma_\mu & t) (\bar{u}_i \gamma^\mu & d_i) \\ (\bar{b}\gamma_\mu T^A & t) (\bar{u}_i \gamma^\mu T^A & d_i) \end{pmatrix}, \quad (85)$$

and two additional complex degrees of freedom can be defined:

$$c_{btud}^{1[I]} = \frac{[\text{Im}]}{\text{Re}} \left\{ \frac{1}{3} C_{ud}^{1(i33i)} + \frac{4}{9} C_{ud}^{8(i33i)} \right\}, \quad c_{btud}^{8[I]} = \frac{[\text{Im}]}{\text{Re}} \left\{ 2 C_{ud}^{1(i33i)} - \frac{1}{3} C_{ud}^{8(i33i)} \right\}. \quad (86)$$

E FCNC degrees of freedom

We now somewhat relax the benchmark flavour symmetry imposed to consider the important case of top-quark FCNC interactions. We therefore assume the $U(2)_q \times U(2)_u \times U(2)_d$ is broken by a small parameter connecting generations 3 and $a \in \{1, 2\}$. In each operator, a quark-antiquark pair mixing these two generations arises at the linear order in this breaking parameter. We restrict ourselves to this order and require the other quark bilinear in a four-quark operator to still satisfy the $U(2)_q \times U(2)_u \times U(2)_d$ symmetry, possibly after a Fierz transformation has been applied. We now construct the degrees of freedom satisfying this condition, operator type by operator type.

E.1 One-light-one-heavy operators

The FCNC operators in this category are trivially obtained from the flavour conserving ones. Note Hermitian couplings $C^{(ji)*} = C^{ij}$ have complex off-diagonal components. The degrees of freedom

Similarly the $\bar{L}\bar{L}\bar{R}R$ operators satisfies $O_{qu}^{1,8(333a)} = O_{qu}^{1,8(33a3)*}$ and $O_{qu}^{1,8(3a33)} = O_{qu}^{1,8(a333)*}$. The $\bar{L}\bar{R}\bar{L}R$ operators have no symmetry of this kind. So, the relevant degrees of freedom are

$$\begin{aligned} c_{qq}^{1[I](333a)} &= \frac{[\text{Im}]\{C_{qq}^{1(333a)}\}}{\text{Re}\{C_{qq}^{1(333a)}\}}, & c_{qu}^{1[I](333a)} &= \frac{[\text{Im}]\{C_{qu}^{1(333a)}\}}{\text{Re}\{C_{qu}^{1(333a)}\}}, & c_{qd}^{1[I](333a)} &= \frac{[\text{Im}]\{C_{qd}^{1(333a)}\}}{\text{Re}\{C_{qd}^{1(333a)}\}}, \\ c_{qq}^{3[I](333a)} &= \frac{[\text{Im}]\{C_{qq}^{3(333a)}\}}{\text{Re}\{C_{qq}^{3(333a)}\}}, & c_{qu}^{8[I](333a)} &= \frac{[\text{Im}]\{C_{qu}^{8(333a)}\}}{\text{Re}\{C_{qu}^{8(333a)}\}}, & c_{qd}^{8[I](333a)} &= \frac{[\text{Im}]\{C_{qd}^{8(333a)}\}}{\text{Re}\{C_{qd}^{8(333a)}\}}, \\ c_{uu}^{[I](333a)} &= \frac{[\text{Im}]\{C_{uu}^{(333a)}\}}{\text{Re}\{C_{uu}^{(333a)}\}}, & c_{qu}^{1[I](3a33)} &= \frac{[\text{Im}]\{C_{qu}^{1(3a33)}\}}{\text{Re}\{C_{qu}^{1(3a33)}\}}, & c_{qd}^{1[I](3a33)} &= \frac{[\text{Im}]\{C_{qd}^{1(3a33)}\}}{\text{Re}\{C_{qd}^{1(3a33)}\}}, \\ & & c_{qu}^{8[I](3a33)} &= \frac{[\text{Im}]\{C_{qu}^{8(3a33)}\}}{\text{Re}\{C_{qu}^{8(3a33)}\}}, & c_{qd}^{8[I](3a33)} &= \frac{[\text{Im}]\{C_{qd}^{8(3a33)}\}}{\text{Re}\{C_{qd}^{8(3a33)}\}}, \end{aligned} \quad (90)$$

$$\begin{aligned} c_{ud}^{1[I](333a)} &= \frac{[\text{Im}]\{C_{ud}^{1(333a)}\}}{\text{Re}\{C_{ud}^{1(333a)}\}}, & c_{quqd}^{1[I](333a)} &= \frac{[\text{Im}]\{C_{quqd}^{1(333a)}\}}{\text{Re}\{C_{quqd}^{1(333a)}\}}, & c_{quqd}^{8[I](333a)} &= \frac{[\text{Im}]\{C_{quqd}^{8(333a)}\}}{\text{Re}\{C_{quqd}^{8(333a)}\}}, \\ c_{ud}^{8[I](333a)} &= \frac{[\text{Im}]\{C_{ud}^{8(333a)}\}}{\text{Re}\{C_{ud}^{8(333a)}\}}, & c_{quqd}^{1[I](33a3)} &= \frac{[\text{Im}]\{C_{quqd}^{1(33a3)}\}}{\text{Re}\{C_{quqd}^{1(33a3)}\}}, & c_{quqd}^{8[I](33a3)} &= \frac{[\text{Im}]\{C_{quqd}^{8(33a3)}\}}{\text{Re}\{C_{quqd}^{8(33a3)}\}}, \\ c_{ud}^{1[I](3a33)} &= \frac{[\text{Im}]\{C_{ud}^{1(3a33)}\}}{\text{Re}\{C_{ud}^{1(3a33)}\}}, & c_{quqd}^{1[I](3a33)} &= \frac{[\text{Im}]\{C_{quqd}^{1(3a33)}\}}{\text{Re}\{C_{quqd}^{1(3a33)}\}}, & c_{quqd}^{8[I](3a33)} &= \frac{[\text{Im}]\{C_{quqd}^{8(3a33)}\}}{\text{Re}\{C_{quqd}^{8(3a33)}\}}, \\ c_{ud}^{8[I](3a33)} &= \frac{[\text{Im}]\{C_{ud}^{8(3a33)}\}}{\text{Re}\{C_{ud}^{8(3a33)}\}}, & c_{quqd}^{1[I](a333)} &= \frac{[\text{Im}]\{C_{quqd}^{1(a333)}\}}{\text{Re}\{C_{quqd}^{1(a333)}\}}, & c_{quqd}^{8[I](a333)} &= \frac{[\text{Im}]\{C_{quqd}^{8(a333)}\}}{\text{Re}\{C_{quqd}^{8(a333)}\}}. \end{aligned} \quad (91)$$

E.4 Three-light-one-heavy operators

Again, we impose here the presence of a quark-antiquark pair satisfying the $U(2)_q \times U(2)_u \times U(2)_d$ symmetry. The suitable $\bar{L}\bar{L}\bar{L}L$ operators satisfy the $O_{qq}^{1,3(3a33)} = O_{qq}^{1,3(ii3a)} = O_{qq}^{1,3(a333)*} = O_{qq}^{1,3(333a)*}$, $O_{qq}^{1,3(333a)} = O_{qq}^{1,3(33a3)} = O_{qq}^{1,3(3a33)} = O_{qq}^{1,3(33a3)*}$ relations. Fierz transformation then lead to

$$\begin{pmatrix} O_{qq}^{1(3a33)} \\ O_{qq}^{1(333a)} \\ O_{qq}^{3(3a33)} \\ O_{qq}^{3(333a)} \end{pmatrix} = \begin{pmatrix} 1 & 1/6 & 0 & 1/2 \\ 0 & 1/6 & 1 & -1/6 \\ 0 & 1 & 0 & 3 \\ 0 & 1 & 0 & -1 \end{pmatrix}^T \begin{pmatrix} (\bar{Q}\gamma_\mu & q_a) (\bar{q}_i\gamma^\mu & q_i) \\ (\bar{Q}\gamma_\mu & \tau^I q_a) (\bar{q}_i\gamma^\mu & \tau^I q_i) \\ (\bar{Q}\gamma_\mu T^A & q_a) (\bar{q}_i\gamma^\mu T^A & q_i) \\ (\bar{Q}\gamma_\mu T^A & \tau^I q_a) (\bar{q}_i\gamma^\mu T^A & \tau^I q_i) \end{pmatrix} \quad (92)$$

and one can thus define the following degrees of freedom:

$$c_{qq}^{1,1[I](3a)} \equiv \frac{[\text{Im}]\{C_{qq}^{1(3a33)}\}}{\text{Re}\{C_{qq}^{1(3a33)}\}} + \frac{1}{6}C_{qq}^{1(333a)} + \frac{1}{2}C_{qq}^{3(333a)}, \quad (93)$$

$$c_{qq}^{3,1[I](3a)} \equiv \frac{[\text{Im}]\{C_{qq}^{3(3a33)}\}}{\text{Re}\{C_{qq}^{3(3a33)}\}} + \frac{1}{6}(C_{qq}^{1(333a)} - C_{qq}^{3(333a)}), \quad (94)$$

$$c_{qq}^{1,8[I](3a)} \equiv \frac{[\text{Im}]\{C_{qq}^{1(333a)}\}}{\text{Re}\{C_{qq}^{1(333a)}\}} + 3C_{qq}^{3(333a)}, \quad (95)$$

$$c_{qq}^{3,8[I](3a)} \equiv \frac{[\text{Im}]\{C_{qq}^{3(333a)}\}}{\text{Re}\{C_{qq}^{3(333a)}\}} - C_{qq}^{1(333a)}, \quad (96)$$

in a way similar to the flavour conserving case. For $\bar{R}\bar{R}\bar{R}R$ operators, one has first:

$$\begin{pmatrix} O_{uu}^{(3a33)} \\ O_{uu}^{(333a)} \end{pmatrix} = \begin{pmatrix} 1 & 1/3 \\ 0 & 2 \end{pmatrix}^T \begin{pmatrix} (\bar{t}\gamma_\mu & u_a) (\bar{u}_i\gamma^\mu & u_i) \\ (\bar{t}\gamma_\mu T^A & u_a) (\bar{u}_i\gamma^\mu T^A & u_i) \end{pmatrix} \quad (97)$$

in the case of the O_{uu} operator whose coefficient with different flavour assignments satisfies the same relations as that of O_{qq} . One thus defines

$$c_{uu}^{1[I](3a)} = \frac{[\text{Im}]\{C_{uu}^{(3a33)}\}}{\text{Re}\{C_{uu}^{(3a33)}\}} + \frac{1}{3}C_{uu}^{(333a)}, \quad (98)$$

$$c_{uu}^{8[I](3a)} = \frac{[\text{Im}]\{2C_{uu}^{(333a)}\}}{\text{Re}\{2C_{uu}^{(333a)}\}},$$

while no Fierzing is required for the definition of the remaining $\bar{R}\bar{R}\bar{R}\bar{R}$ and $\bar{L}\bar{L}\bar{R}\bar{R}$ degrees of freedom:

$$\begin{aligned}
c_{qu}^{1[I](3a)} &= \frac{[\text{Im}]_{\{C_{qu}^{1(3a)}\}}}{\text{Re}\{C_{qu}^{1(3a)}\}}, & c_{qu}^{8[I](3a)} &= \frac{[\text{Im}]_{\{C_{qu}^{8(3a)}\}}}{\text{Re}\{C_{qu}^{8(3a)}\}}, & c_{qd}^{1[I](3a)} &= \frac{[\text{Im}]_{\{C_{qd}^{1(3a)}\}}}{\text{Re}\{C_{qd}^{1(3a)}\}}, \\
c_{ud}^{1[I](3a)} &= \frac{[\text{Im}]_{\{C_{ud}^{1(3a)}\}}}{\text{Re}\{C_{ud}^{1(3a)}\}}, & c_{qu}^{1[I](a3)} &= \frac{[\text{Im}]_{\{C_{qu}^{1(ii3a)}\}}}{\text{Re}\{C_{qu}^{1(ii3a)}\}}, & c_{qd}^{8[I](3a)} &= \frac{[\text{Im}]_{\{C_{qd}^{8(3a)}\}}}{\text{Re}\{C_{qd}^{8(3a)}\}}, \\
c_{ud}^{8[I](3a)} &= \frac{[\text{Im}]_{\{C_{ud}^{8(3a)}\}}}{\text{Re}\{C_{ud}^{8(3a)}\}}, & c_{qu}^{8[I](a3)} &= \frac{[\text{Im}]_{\{C_{qu}^{8(ii3a)}\}}}{\text{Re}\{C_{qu}^{8(ii3a)}\}}, & & &
\end{aligned} \tag{99}$$

E.5 Counting

In total, the counting of FCNC degrees of freedom is as follows:

$$\begin{aligned}
&\text{one-light-one-heavy} && (15 + 15 \text{ CPV}) \times 2 \\
&\text{one-light-one-heavy-two-leptons} && (9 + 9 \text{ CPV}) \times 2 \times 3 \\
&\text{one-light-three-heavy} && (23 + 23 \text{ CPV}) \times 2 \\
&\text{three-light-one-heavy} && (14 + 14 \text{ CPV}) \times 2
\end{aligned}$$

where the factor of two stands for the light quark flavour $a \in \{1, 2\}$, and the factor of three for lepton flavours. One counts 61 CP-even FCNC degrees of freedom without those flavour factors (and 316 including all flavour combinations and CP-odd parameters). Global constraints deriving from direct measurements on a subset of these degrees of freedom were set in Ref. [107].

References

- [1] B. Grzadkowski, M. Iskrzynski, M. Misiak, and J. Rosiek, *Dimension-Six Terms in the Standard Model Lagrangian*, *JHEP* **10** (2010) 085, [arXiv:1008.4884 \[hep-ph\]](#).
- [2] J. A. Aguilar-Saavedra, *A Minimal set of top anomalous couplings*, *Nucl. Phys.* **B812** (2009) 181, [arXiv:0811.3842 \[hep-ph\]](#).
- [3] C. Zhang and S. Willenbrock, *Effective-Field-Theory Approach to Top-Quark Production and Decay*, *Phys. Rev.* **D83** (2011) 034006, [arXiv:1008.3869 \[hep-ph\]](#).
- [4] F. Krauss, S. Kuttimalai, and T. Plehn, *LHC multijet events as a probe for anomalous dimension-six gluon interactions*, *Phys. Rev.* **D95** (2017) 035024, [arXiv:1611.00767 \[hep-ph\]](#).
- [5] J. A. Aguilar-Saavedra, *Effective four-fermion operators in top physics: A Roadmap*, *Nucl. Phys.* **B843** (2011) 638, [Erratum: *Nucl. Phys.*B851,443(2011)], [arXiv:1008.3562 \[hep-ph\]](#).
- [6] C. Zhang, *Effective field theory approach to top-quark decay at next-to-leading order in QCD*, *Phys. Rev.* **D90** (2014) 014008, [arXiv:1404.1264 \[hep-ph\]](#).
- [7] C. Degrande, F. Maltoni, J. Wang, and C. Zhang, *Automatic computations at next-to-leading order in QCD for top-quark flavor-changing neutral processes*, *Phys. Rev.* **D91** (2015) 034024, [arXiv:1412.5594 \[hep-ph\]](#).
- [8] R. Rötsch and M. Schulze, *Constraining couplings of top quarks to the Z boson in $t\bar{t} + Z$ production at the LHC*, *JHEP* **07** (2014) 091, [Erratum: *JHEP*09,132(2015)], [arXiv:1404.1005 \[hep-ph\]](#).
- [9] D. Buarque Franzosi and C. Zhang, *Probing the top-quark chromomagnetic dipole moment at next-to-leading order in QCD*, *Phys. Rev.* **D91** (2015) 114010, [arXiv:1503.08841 \[hep-ph\]](#).
- [10] R. Rötsch and M. Schulze, *Probing top-Z dipole moments at the LHC and ILC*, *JHEP* **08** (2015) 044, [arXiv:1501.05939 \[hep-ph\]](#).

- [11] C. Zhang, *Single Top Production at Next-to-Leading Order in the Standard Model Effective Field Theory*, *Phys. Rev. Lett.* **116** (2016) 162002, arXiv:1601.06163 [hep-ph].
- [12] O. Bessidskaia Bylund, F. Maltoni, I. Tsinikos, E. Vryonidou, and C. Zhang, *Probing top quark neutral couplings in the Standard Model Effective Field Theory at NLO in QCD*, *JHEP* **05** (2016) 052, arXiv:1601.08193 [hep-ph].
- [13] F. Maltoni, E. Vryonidou, and C. Zhang, *Higgs production in association with a top-antitop pair in the Standard Model Effective Field Theory at NLO in QCD*, *JHEP* **10** (2016) 123, arXiv:1607.05330 [hep-ph].
- [14] L. F. Abbott and M. B. Wise, *The Effective Hamiltonian for Nucleon Decay*, *Phys. Rev.* **D22** (1980) 2208.
- [15] R. S. Chivukula and H. Georgi, *Composite Technicolor Standard Model*, *Phys. Lett.* **B188** (1987) 99.
- [16] L. J. Hall and L. Randall, *Weak scale effective supersymmetry*, *Phys. Rev. Lett.* **65** (1990) 2939.
- [17] G. D'Ambrosio, G. F. Giudice, G. Isidori, and A. Strumia, *Minimal flavor violation: An Effective field theory approach*, *Nucl. Phys.* **B645** (2002) 155, arXiv:hep-ph/0207036.
- [18] A. L. Kagan, G. Perez, T. Volansky, and J. Zupan, *General Minimal Flavor Violation*, *Phys. Rev.* **D80** (2009) 076002, arXiv:0903.1794 [hep-ph].
- [19] O. Gedalia, L. Mannelli, and G. Perez, *Covariant Description of Flavor Violation at the LHC*, *Phys. Lett.* **B693** (2010) 301, arXiv:1002.0778 [hep-ph].
- [20] A. Butter, O. J. P. Éboli, J. Gonzalez-Fraile, M. C. Gonzalez-Garcia, T. Plehn, and M. Rauch, *The Gauge-Higgs Legacy of the LHC Run I*, *JHEP* **07** (2016) 152, arXiv:1604.03105 [hep-ph].
- [21] C. W. Murphy, *Statistical approach to Higgs boson couplings in the standard model effective field theory*, *Phys. Rev.* **D97** (2018) 015007, arXiv:1710.02008 [hep-ph].
- [22] S. Di Vita, C. Grojean, G. Panico, M. Riembau, and T. Vantalon, *A global view on the Higgs self-coupling*, *JHEP* **09** (2017) 069, arXiv:1704.01953 [hep-ph].
- [23] A. Falkowski, M. Gonzalez-Alonso, A. Greljo, D. Marzocca, and M. Son, *Anomalous Triple Gauge Couplings in the Effective Field Theory Approach at the LHC*, *JHEP* **02** (2017) 115, arXiv:1609.06312 [hep-ph].
- [24] I. Brivio, J. Gonzalez-Fraile, M. C. Gonzalez-Garcia, and L. Merlo, *The complete HEFT Lagrangian after the LHC Run I*, *Eur. Phys. J.* **C76** (2016) 416, arXiv:1604.06801 [hep-ph].
- [25] C. Englert, R. Kogler, H. Schulz, and M. Spannowsky, *Higgs coupling measurements at the LHC*, *Eur. Phys. J.* **C76** (2016) 393, arXiv:1511.05170 [hep-ph].
- [26] M. L. Mangano, T. Plehn, P. Reimitz, T. Schell, and H.-S. Shao, *Measuring the Top Yukawa Coupling at 100 TeV*, *J. Phys.* **G43** (2016) 035001, arXiv:1507.08169 [hep-ph].
- [27] M. Schulze and Y. Soreq, *Pinning down electroweak dipole operators of the top quark*, *Eur. Phys. J.* **C76** (2016) 466, arXiv:1603.08911 [hep-ph].
- [28] D. Atwood and A. Soni, *Analysis for magnetic moment and electric dipole moment form-factors of the top quark via $e^+e^- \rightarrow t\bar{t}$* , *Phys. Rev.* **D45** (1992) 2405.
- [29] M. Davier, L. Duflot, F. Le Diberder, and A. Rouge, *The Optimal method for the measurement of tau polarization*, *Phys. Lett.* **B306** (1993) 411.

- [30] M. Diehl and O. Nachtmann, *Optimal observables for the measurement of three gauge boson couplings in $e^+e^- \rightarrow W^+W^-$* , *Z. Phys.* **C62** (1994) 397.
- [31] J. Brehmer, K. Cranmer, F. Kling, and T. Plehn, *Better Higgs boson measurements through information geometry*, *Phys. Rev.* **D95** (2017) 073002, [arXiv:1612.05261 \[hep-ph\]](#).
- [32] J. Brehmer, F. Kling, T. Plehn, and T. M. P. Tait, *Better Higgs-CP Tests Through Information Geometry*, (2017), [arXiv:1712.02350 \[hep-ph\]](#).
- [33] A. V. Gritsan, R. Röntsch, M. Schulze, and M. Xiao, *Constraining anomalous Higgs boson couplings to the heavy flavor fermions using matrix element techniques*, *Phys. Rev.* **D94** (2016) 055023, [arXiv:1606.03107 \[hep-ph\]](#).
- [34] G. Abbiendi *et al.* (OPAL), *Measurement of charged current triple gauge boson couplings using W pairs at LEP*, *Eur. Phys. J.* **C33** (2004) 463, [arXiv:hep-ex/0308067](#).
- [35] P. Achard *et al.* (L3), *Measurement of triple gauge boson couplings of the W boson at LEP*, *Phys. Lett.* **B586** (2004) 151, [arXiv:hep-ex/0402036](#).
- [36] S. Schael *et al.* (ALEPH), *Improved measurement of the triple gauge-boson couplings γWW and ZWW in e^+e^- collisions*, *Phys. Lett.* **B614** (2005) 7.
- [37] J. Abdallah *et al.* (DELPHI), *Measurements of CP-conserving Trilinear Gauge Boson Couplings WWV ($V = \gamma, Z$) in e^+e^- Collisions at LEP2*, *Eur. Phys. J.* **C66** (2010) 35, [arXiv:1002.0752 \[hep-ex\]](#).
- [38] G. Aad *et al.* (ATLAS), *Test of CP Invariance in vector-boson fusion production of the Higgs boson using the Optimal Observable method in the ditau decay channel with the ATLAS detector*, *Eur. Phys. J.* **C76** (2016) 658, [arXiv:1602.04516 \[hep-ex\]](#).
- [39] A. Azatov, R. Contino, C. S. Machado, and F. Riva, *Helicity selection rules and noninterference for BSM amplitudes*, *Phys. Rev.* **D95** (2017) 065014, [arXiv:1607.05236 \[hep-ph\]](#).
- [40] J. Alwall, R. Frederix, S. Frixione, V. Hirschi, F. Maltoni, O. Mattelaer, H. S. Shao, T. Stelzer, P. Torrielli, and M. Zaro, *The automated computation of tree-level and next-to-leading order differential cross sections, and their matching to parton shower simulations*, *JHEP* **07** (2014) 079, [arXiv:1405.0301 \[hep-ph\]](#).
- [41] J. Brehmer, A. Freitas, D. Lopez-Val, and T. Plehn, *Pushing Higgs Effective Theory to its Limits*, *Phys. Rev.* **D93** (2016) 075014, [arXiv:1510.03443 \[hep-ph\]](#).
- [42] R. Contino, A. Falkowski, F. Goertz, C. Grojean, and F. Riva, *On the Validity of the Effective Field Theory Approach to SM Precision Tests*, *JHEP* **07** (2016) 144, [arXiv:1604.06444 \[hep-ph\]](#).
- [43] D. de Florian *et al.* (LHC Higgs Cross Section Working Group), *Handbook of LHC Higgs Cross Sections: 4. Deciphering the Nature of the Higgs Sector*, (2016), [10.23731/CYRM-2017-002](#), [arXiv:1610.07922 \[hep-ph\]](#).
- [44] C. Zhang, *Constraining $qqtt$ operators from four-top production: a case for enhanced EFT sensitivity*, *Chin. Phys.* **C42** (2018) 023104, [arXiv:1708.05928 \[hep-ph\]](#).
- [45] A. Buckley, C. Englert, J. Ferrando, D. J. Miller, L. Moore, M. Russell, and C. D. White, *Constraining top quark effective theory in the LHC Run II era*, *JHEP* **04** (2016) 015, [arXiv:1512.03360 \[hep-ph\]](#).
- [46] C. Englert and M. Russell, *Top quark electroweak couplings at future lepton colliders*, *Eur. Phys. J.* **C77** (2017) 535, [arXiv:1704.01782 \[hep-ph\]](#).

- [47] A. Buckley, C. Englert, J. Ferrando, D. J. Miller, L. Moore, M. Russell, and C. D. White, *Global fit of top quark effective theory to data*, *Phys. Rev.* **D92** (2015) 091501, [arXiv:1506.08845 \[hep-ph\]](#).
- [48] R. Barbieri, G. Isidori, J. Jones-Perez, P. Lodone, and D. M. Straub, *U(2) and Minimal Flavour Violation in Supersymmetry*, *Eur. Phys. J.* **C71** (2011) 1725, [arXiv:1105.2296 \[hep-ph\]](#).
- [49] R. Barbieri, D. Buttazzo, F. Sala, and D. M. Straub, *Flavour physics from an approximate U(2)³ symmetry*, *JHEP* **07** (2012) 181, [arXiv:1203.4218 \[hep-ph\]](#).
- [50] V. Cirigliano, M. Gonzalez-Alonso, and M. L. Graesser, *Non-standard Charged Current Interactions: beta decays versus the LHC*, *JHEP* **02** (2013) 046, [arXiv:1210.4553 \[hep-ph\]](#).
- [51] J. Aebischer, A. Crivellin, M. Fael, and C. Greub, *Matching of gauge invariant dimension-six operators for $b \rightarrow s$ and $b \rightarrow c$ transitions*, *JHEP* **05** (2016) 037, [arXiv:1512.02830 \[hep-ph\]](#).
- [52] D. Buttazzo, A. Greljo, G. Isidori, and D. Marzocca, *B-physics anomalies: a guide to combined explanations*, *JHEP* **11** (2017) 044, [arXiv:1706.07808 \[hep-ph\]](#).
- [53] M. Jung and D. M. Straub, *Constraining new physics in $b \rightarrow c\ell\nu$ transitions*, (2018), [arXiv:1801.01112 \[hep-ph\]](#).
- [54] J. P. Lees *et al.* (BaBar), *Measurement of an Excess of $\bar{B} \rightarrow D^{(*)}\tau^-\bar{\nu}_\tau$ Decays and Implications for Charged Higgs Bosons*, *Phys. Rev.* **D88** (2013) 072012, [arXiv:1303.0571 \[hep-ex\]](#).
- [55] R. Aaij *et al.* (LHCb), *Measurement of the ratio of branching fractions $\mathcal{B}(\bar{B}^0 \rightarrow D^{*+}\tau^-\bar{\nu}_\tau)/\mathcal{B}(\bar{B}^0 \rightarrow D^{*+}\mu^-\bar{\nu}_\mu)$* , *Phys. Rev. Lett.* **115** (2015) 111803, [Erratum: *Phys. Rev. Lett.* 115, no. 15, 159901 (2015)], [arXiv:1506.08614 \[hep-ex\]](#).
- [56] M. Huschle *et al.* (Belle), *Measurement of the branching ratio of $\bar{B} \rightarrow D^{(*)}\tau^-\bar{\nu}_\tau$ relative to $\bar{B} \rightarrow D^{(*)}\ell^-\bar{\nu}_\ell$ decays with hadronic tagging at Belle*, *Phys. Rev.* **D92** (2015) 072014, [arXiv:1507.03233 \[hep-ex\]](#).
- [57] Y. Sato *et al.* (Belle), *Measurement of the branching ratio of $\bar{B}^0 \rightarrow D^{*+}\tau^-\bar{\nu}_\tau$ relative to $\bar{B}^0 \rightarrow D^{*+}\ell^-\bar{\nu}_\ell$ decays with a semileptonic tagging method*, *Phys. Rev.* **D94** (2016) 072007, [arXiv:1607.07923 \[hep-ex\]](#).
- [58] S. Hirose *et al.* (Belle), *Measurement of the τ lepton polarization and $R(D^*)$ in the decay $\bar{B} \rightarrow D^*\tau^-\bar{\nu}_\tau$* , *Phys. Rev. Lett.* **118** (2017) 211801, [arXiv:1612.00529 \[hep-ex\]](#).
- [59] R. Alonso, B. Grinstein, and J. Martin Camalich, *Lifetime of B_c^- Constrains Explanations for Anomalies in $B \rightarrow D^{(*)}\tau\nu$* , *Phys. Rev. Lett.* **118** (2017) 081802, [arXiv:1611.06676 \[hep-ph\]](#).
- [60] G. Isidori, *Flavor physics and CP violation*, in *Proceedings, 2012 European School of High-Energy Physics (ESHEP 2012): La Pommeraye, Anjou, France, June 06-19, 2012* (2014) pp. 69–105, [arXiv:1302.0661 \[hep-ph\]](#).
- [61] W. Altmannshofer and D. M. Straub, *Implications of $b \rightarrow s$ measurements*, in *Proceedings, 50th Rencontres de Moriond Electroweak Interactions and Unified Theories: La Thuile, Italy, March 14-21, 2015* (2015) pp. 333–338, [arXiv:1503.06199 \[hep-ph\]](#).
- [62] S. Descotes-Genon, L. Hofer, J. Matias, and J. Virto, *Global analysis of $b \rightarrow s\ell\ell$ anomalies*, *JHEP* **06** (2016) 092, [arXiv:1510.04239 \[hep-ph\]](#).
- [63] J. Brod, A. Greljo, E. Stamou, and P. Uttayarat, *Probing anomalous $t\bar{t}Z$ interactions with rare meson decays*, *JHEP* **02** (2015) 141, [arXiv:1408.0792 \[hep-ph\]](#).

- [64] A. Greljo and D. Marzocca, *High- p_T dilepton tails and flavor physics*, *Eur. Phys. J.* **C77** (2017) 548, [arXiv:1704.09015 \[hep-ph\]](#).
- [65] D. A. Faroughy, A. Greljo, and J. F. Kamenik, *Confronting lepton flavor universality violation in B decays with high- p_T tau lepton searches at LHC*, *Phys. Lett.* **B764** (2017) 126, [arXiv:1609.07138 \[hep-ph\]](#).
- [66] M. Farina, G. Panico, D. Pappadopulo, J. T. Ruderman, R. Torre, and A. Wulzer, *Energy helps accuracy: electroweak precision tests at hadron colliders*, *Phys. Lett.* **B772** (2017) 210, [arXiv:1609.08157 \[hep-ph\]](#).
- [67] S. Alioli, M. Farina, D. Pappadopulo, and J. T. Ruderman, *Precision Probes of QCD at High Energies*, *JHEP* **07** (2017) 097, [arXiv:1706.03068 \[hep-ph\]](#).
- [68] S. Alioli, M. Farina, D. Pappadopulo, and J. T. Ruderman, *Catching a New Force by the Tail*, (2017), [arXiv:1712.02347 \[hep-ph\]](#).
- [69] N. Greiner, S. Willenbrock, and C. Zhang, *Effective Field Theory for Nonstandard Top Quark Couplings*, *Phys. Lett.* **B704** (2011) 218, [arXiv:1104.3122 \[hep-ph\]](#).
- [70] C. Zhang, N. Greiner, and S. Willenbrock, *Constraints on Non-standard Top Quark Couplings*, *Phys. Rev.* **D86** (2012) 014024, [arXiv:1201.6670 \[hep-ph\]](#).
- [71] K. Hagiwara, S. Ishihara, R. Szalapski, and D. Zeppenfeld, *Low-energy effects of new interactions in the electroweak boson sector*, *Phys. Rev.* **D48** (1993) 2182.
- [72] J. de Blas, M. Chala, and J. Santiago, *Renormalization Group Constraints on New Top Interactions from Electroweak Precision Data*, *JHEP* **09** (2015) 189, [arXiv:1507.00757 \[hep-ph\]](#).
- [73] F. Feruglio, P. Paradisi, and A. Pattori, *Revisiting Lepton Flavor Universality in B Decays*, *Phys. Rev. Lett.* **118** (2017) 011801, [arXiv:1606.00524 \[hep-ph\]](#).
- [74] F. Feruglio, P. Paradisi, and A. Pattori, *On the Importance of Electroweak Corrections for B Anomalies*, *JHEP* **09** (2017) 061, [arXiv:1705.00929 \[hep-ph\]](#).
- [75] A. Efrati, A. Falkowski, and Y. Soreq, *Electroweak constraints on flavorful effective theories*, *JHEP* **07** (2015) 018, [arXiv:1503.07872 \[hep-ph\]](#).
- [76] D. A. Dicus, *Neutron Electric Dipole Moment From Charged Higgs Exchange*, *Phys.Rev.* **D41** (1990) 999.
- [77] S. Weinberg, *Larger Higgs Exchange Terms in the Neutron Electric Dipole Moment*, *Phys. Rev. Lett.* **63** (1989) 2333.
- [78] E. Braaten, C.-S. Li, and T.-C. Yuan, *The Evolution of Weinberg's Gluonic CP Violation Operator*, *Phys. Rev. Lett.* **64** (1990) 1709.
- [79] G. Boyd, A. K. Gupta, S. P. Trivedi, and M. B. Wise, *Effective Hamiltonian for the Electric Dipole Moment of the Neutron*, *Phys.Lett.* **B241** (1990) 584.
- [80] J. F. Kamenik, M. Papucci, and A. Weiler, *Constraining the dipole moments of the top quark*, *Phys. Rev.* **D85** (2012) 071501, [Erratum: *Phys. Rev.*D88,no.3,039903(2013)], [arXiv:1107.3143 \[hep-ph\]](#).
- [81] J. Brod, U. Haisch, and J. Zupan, *Constraints on CP-violating Higgs couplings to the third generation*, *JHEP* **11** (2013) 180, [arXiv:1310.1385 \[hep-ph\]](#).
- [82] S. M. Barr and A. Zee, *Electric Dipole Moment of the Electron and of the Neutron*, *Phys. Rev. Lett.* **65** (1990) 21.

- [83] J. Gunion and D. Wyler, *Inducing a large neutron electric dipole moment via a quark chromoelectric dipole moment*, *Phys.Lett.* **B248** (1990) 170.
- [84] T. Abe, J. Hisano, T. Kitahara, and K. Tobioka, *Gauge invariant Barr-Zee type contributions to fermionic EDMs in the two-Higgs doublet models*, *JHEP* **1401** (2014) 106, [arXiv:1311.4704 \[hep-ph\]](#).
- [85] M. Jung and A. Pich, *Electric Dipole Moments in Two-Higgs-Doublet Models*, *JHEP* **04** (2014) 076, [arXiv:1308.6283 \[hep-ph\]](#).
- [86] W. Dekens and J. de Vries, *Renormalization Group Running of Dimension-Six Sources of Parity and Time-Reversal Violation*, *JHEP* **1305** (2013) 149, [arXiv:1303.3156 \[hep-ph\]](#).
- [87] R. Alonso, E. E. Jenkins, A. V. Manohar, and M. Trott, *Renormalization Group Evolution of the Standard Model Dimension Six Operators III: Gauge Coupling Dependence and Phenomenology*, *JHEP* **04** (2014) 159, [arXiv:1312.2014 \[hep-ph\]](#).
- [88] V. Cirigliano, W. Dekens, J. de Vries, and E. Mereghetti, *Constraining the top-Higgs sector of the Standard Model Effective Field Theory*, *Phys. Rev.* **D94** (2016) 034031, [arXiv:1605.04311 \[hep-ph\]](#).
- [89] S. Alioli, V. Cirigliano, W. Dekens, J. de Vries, and E. Mereghetti, *Right-handed charged currents in the era of the Large Hadron Collider*, *JHEP* **05** (2017) 086, [arXiv:1703.04751 \[hep-ph\]](#).
- [90] D. A. Demir, M. Pospelov, and A. Ritz, *Hadronic EDMs, the Weinberg operator, and light gluinos*, *Phys. Rev. D* **67** (2003) 015007, [arXiv:hep-ph/0208257](#).
- [91] J. de Vries, R. G. E. Timmermans, E. Mereghetti, and U. van Kolck, *The Nucleon Electric Dipole Form Factor From Dimension-Six Time-Reversal Violation*, *Phys. Lett.* **B695** (2011) 268, [arXiv:1006.2304 \[hep-ph\]](#).
- [92] Y. T. Chien, V. Cirigliano, W. Dekens, J. de Vries, and E. Mereghetti, *Direct and indirect constraints on CP-violating Higgs-quark and Higgs-gluon interactions*, *JHEP* **02** (2016) 011, [JHEP02,011(2016)], [arXiv:1510.00725 \[hep-ph\]](#).
- [93] J. Pendlebury *et al.*, *Revised experimental upper limit on the electric dipole moment of the neutron*, *Phys. Rev.* **D92** (2015) 092003, [arXiv:1509.04411 \[hep-ex\]](#).
- [94] C. A. Baker, D. D. Doyle, P. Geltenbort, K. Green, M. G. D. van der Grinten, *et al.*, *An Improved experimental limit on the electric dipole moment of the neutron*, *Phys. Rev. Lett.* **97** (2006) 131801, [arXiv:hep-ex/0602020](#).
- [95] J. Baron *et al.* (ACME Collaboration), *Order of Magnitude Smaller Limit on the Electric Dipole Moment of the Electron*, *Science* **343** (2014) 269, [arXiv:1310.7534 \[physics.atom-ph\]](#).
- [96] V. Cirigliano, W. Dekens, J. de Vries, and E. Mereghetti, *Is there room for CP violation in the top-Higgs sector?*, *Phys. Rev.* **D94** (2016) 016002, [arXiv:1603.03049 \[hep-ph\]](#).
- [97] K. Fuyuto and M. Ramsey-Musolf, *Top Down Electroweak Dipole Operators*, (2017), [arXiv:1706.08548 \[hep-ph\]](#).
- [98] M. Benzke, S. J. Lee, M. Neubert, and G. Paz, *Long-Distance Dominance of the CP Asymmetry in $B \rightarrow X_{s,d} + \gamma$ Decays*, *Phys. Rev. Lett.* **106** (2011) 141801, [arXiv:1012.3167 \[hep-ph\]](#).
- [99] Y. Amhis *et al.* (HFLAV), *Averages of b-hadron, c-hadron, and τ -lepton properties as of summer 2016*, *Eur. Phys. J.* **C77** (2017) 895, [arXiv:1612.07233 \[hep-ex\]](#).

- [100] B. Grzadkowski and M. Misiak, *Anomalous Wtb coupling effects in the weak radiative B -meson decay*, *Phys. Rev. D* **78** (2008) 077501, [arXiv:0802.1413 \[hep-ph\]](#).
- [101] J. Drobnak, S. Fajfer, and J. F. Kamenik, *Probing anomalous tWb interactions with rare B decays*, *Nucl. Phys.* **B855** (2012) 82, [arXiv:1109.2357 \[hep-ph\]](#).
- [102] J. Drobnak, S. Fajfer, and J. F. Kamenik, *Interplay of $t \rightarrow bW$ Decay and B_q Meson Mixing in Minimal Flavor Violating Models*, *Phys. Lett. B* **701** (2011) 234, [arXiv:1102.4347 \[hep-ph\]](#).
- [103] M. Aaboud *et al.* (ATLAS), *Analysis of the Wtb vertex from the measurement of triple-differential angular decay rates of single top quarks produced in the t -channel at $\sqrt{s} = 8$ TeV with the ATLAS detector*, *JHEP* **12** (2017) 017, [arXiv:1707.05393 \[hep-ex\]](#).
- [104] C. Degrande, C. Duhr, B. Fuks, D. Grellscheid, O. Mattelaer, and T. Reiter, *UFO - The Universal FeynRules Output*, *Comput. Phys. Commun.* **183** (2012) 1201, [arXiv:1108.2040 \[hep-ph\]](#).
- [105] I. Brivio, Y. Jiang, and M. Trott, *The SMEFTsim package, theory and tools*, *JHEP* **12** (2017) 070, [arXiv:1709.06492 \[hep-ph\]](#).
- [106] A. Alloul, N. D. Christensen, C. Degrande, C. Duhr, and B. Fuks, *FeynRules 2.0 - A complete toolbox for tree-level phenomenology*, *Comput. Phys. Commun.* **185** (2014) 2250, [arXiv:1310.1921 \[hep-ph\]](#).
- [107] G. Durieux, F. Maltoni, and C. Zhang, *Global approach to top-quark flavor-changing interactions*, *Phys. Rev.* **D91** (2015) 074017, [arXiv:1412.7166 \[hep-ph\]](#).

		$pp \rightarrow t\bar{t}$	$pp \rightarrow t\bar{t}b\bar{b}$	$pp \rightarrow t\bar{t}t\bar{t}$	$pp \rightarrow t\bar{t}e^+\nu$	$pp \rightarrow t\bar{t}e^+e^-$	$pp \rightarrow t\bar{t}\gamma$	$pp \rightarrow t\bar{t}h$
SM	sm	5.2×10^2 pb	1.9 pb	0.0098 pb	0.02 pb	0.016 pb	1.4 pb	0.4 pb
c_{QQ}^1	cQq1	-0.25	-1.9	-1×10^2		-1.6	-0.67	-0.71
c_{QQ}^8	cQQ8	-0.16	-3.2	-34		-0.91	-0.5	-0.27
c_{Qt}^1	cQt1	-0.15	-5.6	1×10^2		-0.76	-0.19	-0.55
c_{Qt}^8	cQt8	-0.053	-1.8	-41		-0.18	-0.095	-0.15
c_{Qb}^1	cQb1	-0.0055	0.72	-0.052		-0.015	-0.007	-0.026
c_{Qb}^8	cQb8	0.14	3.9	0.12		0.35	0.16	0.56
c_{tt}^1	ctt1			-1.8×10^2				
c_{tb}^1	ctb1	-0.0095	0.46	-0.059		-0.02	-0.026	-0.039
c_{tb}^8	ctb8	0.13	3.5	0.11		0.26	0.31	0.56
c_{QtQb}^1	cQtQb1							
c_{QtQb}^8	cQtQb8							
c_{QtQb}^{1I}	cQtQb1I							
c_{QtQb}^{8I}	cQtQb8I							
$c_{Qq}^{3,8}$	cQq83	2.7	-0.11	4.7	-85	-20	8.5	15
$c_{Qq}^{1,8}$	cQq81	12	7.1	25	2.6×10^2	71	40	75
c_{Qu}^8	cQu8	13	8.2	27	2.6×10^2	62	51	74
c_{Qu}^1	cQu1	7.4	4.4	18		21	41	44
c_{tu}^8	ctu8	7.4	3	16		14	22	45
c_{td}^8	ctd8	5	3	11		17	7.3	29
c_{td}^1	ctd1	5	2.1	10		12	10	28
$c_{Qq}^{3,1}$	cQq13	3.3	3	5.8	1.1×10^2	22	11	18
$c_{Qq}^{1,1}$	cQq11	0.94	-1.4	-7.7	-5.9	-5	3	5.4
c_{tq}^1	ctq1	0.65	2.4	-7.9	8.7	0.84	3.7	4.8
c_{Qu}^1	cQu1	0.57	1.5	-5.2		1.5	2.9	4.3
c_{tu}^1	ctu1	1.1	-0.29	-3.8		2.3	3.3	6.6
c_{td}^1	ctd1	-0.19	0.55	-4		-0.66	-0.3	-1.4
c_{td}^8	ctd1	-0.37	-1.3	-5		-0.91	-1.3	-2.1
$c_{t\varphi}$	ctp		-0.00035	-9.1	-0.034	-0.0093		-1.2×10^2
$c_{\varphi Q}^-$	cpQM	-0.063	1	-41	-0.76	-1×10^2	-0.13	-0.29
$c_{\varphi Q}^3$	cpQ3	0.68	22	0.065	0.46	3.7	1.5	1.8
$c_{\varphi t}$	cpt	-0.024	2.8	42	-0.36	68	-0.058	-0.16
$c_{\varphi tb}$	cptb							
c_{tW}	ctW	0.98	1	-34	13	1.1	69	9.4
c_{tZ}	ctZ	-0.54	0.028	27	-0.048	-3.6	-55	-4.3
c_{bW}	cbW							
c_{tG}	ctG	2.7×10^2	2.5×10^2	3.8×10^2	2.4×10^2	3.1×10^2	2.4×10^2	8.4×10^2
$c_{t\varphi}^I$	ctpI		-7.3×10^{-7}	0.045	-0.00064	-0.00029		0.045
$c_{\varphi tb}^I$	cptbI							
c_{tW}^I	ctWI	4.8×10^{-6}	0.032	-1.6	-0.19	0.29	0.91	0.031
c_{tZ}^I	ctZI	-1.4×10^{-6}	0.1	-1.2	0.0098	3.2	-0.56	-0.057
c_{bW}^I	cbWI							
c_{tG}^I	ctGI	-0.00098	0.48	0.66	0.031	-0.7	0.019	-2.4
$c_{Ql}^{3(1)}$	cQl31				0.011	0.06		
$c_{Ql}^{-(1)}$	cQlM1				-0.0062	-9.8		
$c_{Qe}^{(1)}$	cQe1					-1.5		
$c_{tl}^{(1)}$	ctl1				-0.0023	-3.6		
$c_{te}^{(1)}$	cte1					-6.7		
$c_{tl}^{S(1)}$	ctlS1							
$c_{tl}^{T(1)}$	ctlT1							
$c_{bl}^{S(1)}$	ctlS1							
$c_{bl}^{SI(1)}$	ctlSI1							
$c_{tl}^{TI(1)}$	ctlTI1							
$c_{bl}^{SI(1)}$	ctlSI1							
c_{tQqu}^1	ctQqu1							
c_{tQqu}^8	ctQqu8							
c_{bQqd}^1	cbQqd1							
c_{bQqd}^8	cbQqd8							
c_{Qtqd}^1	cQtqd1							
c_{Qtqd}^8	cQtqd8							
c_{Qbqu}^1	cQbqu1							
c_{Qbqu}^8	cQbqu8							
c_{btud}^1	cbtud1							
c_{btud}^8	cbtud8							
c_{tQqu}^{1I}	ctQqu1I							
c_{tQqu}^{8I}	ctQqu8I							
c_{bQqd}^{1I}	cbQqd1I							
c_{bQqd}^{8I}	cbQqd8I							
c_{Qtqd}^{1I}	cQtqd1I							
c_{Qtqd}^{8I}	cQtqd8I							
c_{Qbqu}^{1I}	cQbqu1I							
c_{Qbqu}^{8I}	cQbqu8I							
c_{btud}^{1I}	cbtud1I							
c_{btud}^{8I}	cbtud8I							

Table 10: Linear dependences on the various degrees of freedom of total top pair production rates at the 13 TeV LHC. For convenience, numerical values for the $S_j^k / \sum_l B_l^k$ ratios are provided in permil. Absolute SM rates (i.e. $\sum_l B_l^k$) are also quoted in picobarns. LO simulation at the parton level, the five-flavour scheme, NNPDF2.3LO1, running renormalization and factorization scales are used. Simple $p_T > 20$ GeV, $|\eta| < 2.5$, $\Delta R > 0.4$ cuts are imposed on (b -)jets, charged leptons and photons. As input parameters, $m_t = 172$ GeV (all other fermion masses and Yukawa couplings are set to zero) and $m_h = 125$ GeV are notably employed. Monte Carlo uncertainties are of the order of 15%, but outliers are expected given the number of quantity evaluated.

SM	sm	$pp \rightarrow tj$	$pp \rightarrow te^{-}\bar{\nu}$	$pp \rightarrow tje^{+}e^{-}$	$pp \rightarrow tj\gamma$	$pp \rightarrow tjh$
		55 pb	2.5 pb	0.0054 pb	0.39 pb	0.016 pb
c_{8Q}^1	cQQ1					
c_{8Q}^2	cQQ8					
c_{8t}^1	cQt1					
c_{8t}^2	cQt8					
c_{8b}^1	cQb1					
c_{8b}^2	cQb8					
c_{8t}^1	ctt1					
c_{8b}^1	ctb1					
c_{8b}^2	ctb8					
c_{8tQb}^1	cQtQb1					
c_{8tQb}^2	cQtQb8					
c_{8tQb}^I	cQtQb1I					
c_{8tQb}^{SI}	cQtQb8I					
$c_{8Q}^{3,8}$	cQq83	-3.4×10^{-15}		-6.4×10^{-15}	-5.2×10^{-15}	-4.1×10^{-15}
$c_{8q}^{1,8}$	cQq81					
c_{8q}^2	ctq8					
c_{8q}^3	cQu8					
c_{8u}^1	ctu8					
c_{8d}^1	cQd8					
c_{8d}^2	ctd8					
$c_{8q}^{3,1}$	cQq13	-3.8×10^2		-7.9×10^2	-6.1×10^2	-4.6×10^2
$c_{8q}^{1,1}$	cQq11					
c_{8q}^1	ctq1					
c_{8u}^1	cQu1					
c_{8u}^2	ctu1					
c_{8d}^1	cQd1					
c_{8d}^2	ctd1					
$c_{t\varphi}$	ctp					-68
$c_{\varphi Q}^-$	cpQM			21		
$c_{\varphi Q}^3$	cpQ3	1.2×10^2	1.2×10^2	2.2×10^2	1.2×10^2	1.3×10^2
$c_{\varphi t}$	cpt			5.2		
$c_{\varphi tb}$	cptb					
c_{tW}	ctW	84	-76	45	50	9.1×10^2
c_{tZ}	ctZ			-10	-6	
c_{bW}	cbW					
c_{tG}	ctG		59			
$c_{t\varphi}^I$	ctpI					-0.21
$c_{\varphi tb}^I$	cptbI					
c_{tW}^I	ctWI	1.6×10^{-16}	-1.4	0.47	0.022	-0.13
c_{tZ}^I	ctZI			-0.87	0.67	
c_{bW}^I	cbWI					
c_{tG}^I	ctGI		0.4			
$c_{QI}^{3(1)}$	cQ131		4.1	6		
$c_{QI}^{-(1)}$	cQ1M1			2.2		
$c_{Qe}^{(1)}$	cQe1			-0.39		
$c_{tI}^{(1)}$	ct11			-0.036		
$c_{te}^{(1)}$	cte1			0.064		
$c_{tI}^{S(1)}$	ct1S1					
$c_{tI}^{T(1)}$	ct1T1					
$c_{bI}^{S(1)}$	cb1S1					
$c_{tI}^{SI(1)}$	ct1SI1					
$c_{tI}^{TI(1)}$	ct1TI1					
$c_{bI}^{SI(1)}$	cb1SI1					
c_{8tQu}^1	ctQqu1					
c_{8tQu}^2	ctQqu8					
c_{8bQqd}^1	cbQqd1					
c_{8bQqd}^2	cbQqd8					
c_{8tQqd}^1	cQtqd1					
c_{8tQqd}^2	cQtqd8					
c_{8bqu}^1	cQbqu1					
c_{8bqu}^2	cQbqu8					
c_{8btud}^1	cbtud1					
c_{8btud}^2	cbtud8					
c_{8tQu}^I	ctQqu1I					
c_{8tQu}^{SI}	ctQqu8I					
c_{8bQqd}^I	cbQqd1I					
c_{8bQqd}^{SI}	cbQqd8I					
c_{8tQqd}^I	cQtqd1I					
c_{8tQqd}^{SI}	cQtqd8I					
c_{8bqu}^I	cQbqu1I					
c_{8bqu}^{SI}	cQbqu8I					
c_{8btud}^I	cbtud1I					
c_{8btud}^{SI}	cbtud8I					

Table 11: Same as Table 10, for single top production processes.

	δ_{51}	δ_{52}	δ_{53}	δ_{54}	δ_{55}	δ_{56}	δ_{57}	δ_{58}	δ_{59}	δ_{60}	δ_{61}	δ_{62}	δ_{63}	δ_{64}	δ_{65}	δ_{66}	δ_{67}	δ_{68}	δ_{69}	δ_{70}	δ_{71}	δ_{72}	δ_{73}	δ_{74}	δ_{75}	δ_{76}	δ_{77}	δ_{78}	δ_{79}	δ_{80}	δ_{81}	δ_{82}	δ_{83}	δ_{84}	δ_{85}	δ_{86}	δ_{87}	δ_{88}	δ_{89}	δ_{90}	δ_{91}	δ_{92}	δ_{93}	δ_{94}	δ_{95}	δ_{96}	δ_{97}	δ_{98}	δ_{99}	δ_{100}				
δ_{10}	0.07	0.05	0.03	0.06	0.08	0.09	0.04	0.07	0.05	0.06	0.08	0.09	0.04	0.07	0.05	0.06	0.08	0.09	0.04	0.07	0.05	0.06	0.08	0.09	0.04	0.07	0.05	0.06	0.08	0.09	0.04	0.07	0.05	0.06	0.08	0.09	0.04	0.07	0.05	0.06	0.08	0.09	0.04	0.07	0.05	0.06	0.08	0.09						
δ_{11}	0.07	0.05	0.03	0.06	0.08	0.09	0.04	0.07	0.05	0.06	0.08	0.09	0.04	0.07	0.05	0.06	0.08	0.09	0.04	0.07	0.05	0.06	0.08	0.09	0.04	0.07	0.05	0.06	0.08	0.09	0.04	0.07	0.05	0.06	0.08	0.09	0.04	0.07	0.05	0.06	0.08	0.09	0.04	0.07	0.05	0.06	0.08	0.09	0.04	0.07	0.05	0.06	0.08	0.09

Table 12: Quadratic dependence on the various degrees of freedom of the total $pp \rightarrow t\bar{t}$ rate. For conveniences, numerical values for $S_{ij}^b / \sum_l B_l^b$ are quoted in permil. Numerical values smaller than 10^{-5} are omitted. For more details see the legend of Table 10.

μ_j	μ_{j+1}	μ_{j+2}	μ_{j+3}	μ_{j+4}	μ_{j+5}	μ_{j+6}	μ_{j+7}	μ_{j+8}	μ_{j+9}	μ_{j+10}	μ_{j+11}	μ_{j+12}	μ_{j+13}	μ_{j+14}	μ_{j+15}	μ_{j+16}	μ_{j+17}	μ_{j+18}	μ_{j+19}	μ_{j+20}	μ_{j+21}	μ_{j+22}	μ_{j+23}	μ_{j+24}	μ_{j+25}	μ_{j+26}	μ_{j+27}	μ_{j+28}	μ_{j+29}	μ_{j+30}	μ_{j+31}	μ_{j+32}	μ_{j+33}	μ_{j+34}	μ_{j+35}	μ_{j+36}	μ_{j+37}	μ_{j+38}	μ_{j+39}	μ_{j+40}	μ_{j+41}	μ_{j+42}	μ_{j+43}	μ_{j+44}	μ_{j+45}	μ_{j+46}	μ_{j+47}	μ_{j+48}	μ_{j+49}	μ_{j+50}	μ_{j+51}	μ_{j+52}	μ_{j+53}	μ_{j+54}	μ_{j+55}	μ_{j+56}	μ_{j+57}	μ_{j+58}	μ_{j+59}	μ_{j+60}	μ_{j+61}	μ_{j+62}	μ_{j+63}	μ_{j+64}	μ_{j+65}	μ_{j+66}	μ_{j+67}	μ_{j+68}	μ_{j+69}	μ_{j+70}	μ_{j+71}	μ_{j+72}	μ_{j+73}	μ_{j+74}	μ_{j+75}	μ_{j+76}	μ_{j+77}	μ_{j+78}	μ_{j+79}	μ_{j+80}	μ_{j+81}	μ_{j+82}	μ_{j+83}	μ_{j+84}	μ_{j+85}	μ_{j+86}	μ_{j+87}	μ_{j+88}	μ_{j+89}	μ_{j+90}	μ_{j+91}	μ_{j+92}	μ_{j+93}	μ_{j+94}	μ_{j+95}	μ_{j+96}	μ_{j+97}	μ_{j+98}	μ_{j+99}	μ_{j+100}	μ_{j+101}	μ_{j+102}	μ_{j+103}	μ_{j+104}	μ_{j+105}	μ_{j+106}	μ_{j+107}	μ_{j+108}	μ_{j+109}	μ_{j+110}	μ_{j+111}	μ_{j+112}	μ_{j+113}	μ_{j+114}	μ_{j+115}	μ_{j+116}	μ_{j+117}	μ_{j+118}	μ_{j+119}	μ_{j+120}	μ_{j+121}	μ_{j+122}	μ_{j+123}	μ_{j+124}	μ_{j+125}	μ_{j+126}	μ_{j+127}	μ_{j+128}	μ_{j+129}	μ_{j+130}	μ_{j+131}	μ_{j+132}	μ_{j+133}	μ_{j+134}	μ_{j+135}	μ_{j+136}	μ_{j+137}	μ_{j+138}	μ_{j+139}	μ_{j+140}	μ_{j+141}	μ_{j+142}	μ_{j+143}	μ_{j+144}	μ_{j+145}	μ_{j+146}	μ_{j+147}	μ_{j+148}	μ_{j+149}	μ_{j+150}	μ_{j+151}	μ_{j+152}	μ_{j+153}	μ_{j+154}	μ_{j+155}	μ_{j+156}	μ_{j+157}	μ_{j+158}	μ_{j+159}	μ_{j+160}	μ_{j+161}	μ_{j+162}	μ_{j+163}	μ_{j+164}	μ_{j+165}	μ_{j+166}	μ_{j+167}	μ_{j+168}	μ_{j+169}	μ_{j+170}	μ_{j+171}	μ_{j+172}	μ_{j+173}	μ_{j+174}	μ_{j+175}	μ_{j+176}	μ_{j+177}	μ_{j+178}	μ_{j+179}	μ_{j+180}	μ_{j+181}	μ_{j+182}	μ_{j+183}	μ_{j+184}	μ_{j+185}	μ_{j+186}	μ_{j+187}	μ_{j+188}	μ_{j+189}	μ_{j+190}	μ_{j+191}	μ_{j+192}	μ_{j+193}	μ_{j+194}	μ_{j+195}	μ_{j+196}	μ_{j+197}	μ_{j+198}	μ_{j+199}	μ_{j+200}
0.00	0.01	0.02	0.03	0.04	0.05	0.06	0.07	0.08	0.09	0.10	0.11	0.12	0.13	0.14	0.15	0.16	0.17	0.18	0.19	0.20	0.21	0.22	0.23	0.24	0.25	0.26	0.27	0.28	0.29	0.30	0.31	0.32	0.33	0.34	0.35	0.36	0.37	0.38	0.39	0.40	0.41	0.42	0.43	0.44	0.45	0.46	0.47	0.48	0.49	0.50	0.51	0.52	0.53	0.54	0.55	0.56	0.57	0.58	0.59	0.60	0.61	0.62	0.63	0.64	0.65	0.66	0.67	0.68	0.69	0.70	0.71	0.72	0.73	0.74	0.75	0.76	0.77	0.78	0.79	0.80	0.81	0.82	0.83	0.84	0.85	0.86	0.87	0.88	0.89	0.90	0.91	0.92	0.93	0.94	0.95	0.96	0.97	0.98	0.99	1.00																																																																																																				

Table 16: Quadratic dependence on the various degrees of freedom of the total $pp \rightarrow t\bar{t}h$ rate. For conveniences, numerical values for $S_{ij}^k / \sum_l B_l^k$ are quoted in permil. For more details see the legend of Table 10.

